




BRIEF DEFINITIVE REPORT

T reg cell–intrinsic requirements for ST2 signaling in health and neuroinflammation

Saskia Hemmers^{1,2} , Michail Schizas^{1,2} , and Alexander Y. Rudensky^{1,2} 

ST2, the receptor for the alarmin IL-33, is expressed by a subset of regulatory T (T reg) cells residing in nonlymphoid tissues, and these cells can potently expand upon provision of exogenous IL-33. Whether the accumulation and residence of T reg cells in tissues requires their cell-intrinsic expression of and signaling by ST2, or whether indirect IL-33 signaling acting on other cells suffices, has been a matter of contention. Here, we report that ST2 expression on T reg cells is largely dispensable for their accumulation and residence in nonlymphoid organs, including the visceral adipose tissue (VAT), even though cell-intrinsic sensing of IL-33 promotes type 2 cytokine production by VAT-residing T reg cells. In addition, we uncovered a novel ST2-dependent role for T reg cells in limiting the size of IL-17A–producing $\gamma\delta$ T cells in the CNS in a mouse model of neuroinflammation, experimental autoimmune encephalomyelitis (EAE). Finally, ST2 deficiency limited to T reg cells led to disease exacerbation in EAE.

Introduction

Regulatory T (T reg) cells are a specialized subset of CD4⁺ T cells that express the lineage-defining transcription factor Foxp3. They are essential for maintenance of immune tolerance, as loss of Foxp3, and therefore loss of T reg cells, leads to early-onset catastrophic multiorgan autoimmune disease and premature death in mice and humans (Bennett et al., 2001; Brunkow et al., 2001; Fontenot et al., 2003; Khattri et al., 2003; Kim et al., 2007; Lahl et al., 2007; Sakaguchi et al., 1995). As potent immune suppressors, T reg cells modulate a wide variety of immune cells and contribute to diverse pathologies including autoimmunity and cancer (Josefowicz et al., 2012; Sakaguchi et al., 2020). More recently, T reg cells have been shown to perform essential functions in maintenance of tissue tolerance by promoting tissue homeostasis and regeneration in nonlymphoid tissues, including lung (Arpaia et al., 2015), skin (Ali et al., 2017), muscle (Burzyn et al., 2013), adipose tissue (Cipolletta et al., 2012; Feuerer et al., 2009; Vasanthakumar et al., 2015), and the central nervous system (CNS; Dombrowski et al., 2017; Ito et al., 2019). These nonlymphoid tissue T reg cells are thought to promote tissue repair by sensing tissue damage in situ via soluble factors including the proinflammatory cytokine IL-18 and the alarmin IL-33, at least in part independent of TCR signaling (Arpaia et al., 2015; Burzyn et al., 2013). A major component of this tissue regenerative pathway in T reg cells is the production of the prorepair factor amphiregulin (Areg; Arpaia et al., 2015; Burzyn

et al., 2013; Ito et al., 2019), but other mechanisms remain to be explored.

T reg cells residing in nonlymphoid tissues are highly enriched for cells with an effector phenotype (Panduro et al., 2016). A subset of those is characterized by expression of the IL-1R family member ST2 (encoded by *Il1rl1*), the receptor for the alarmin IL-33. These cells were recently shown to develop from precursors found in spleen and LNs in a basic leucine zipper transcription factor, ATF-like (BATF)–dependent manner (Delacher et al., 2020; Miragaia et al., 2019). IL-33 is a member of the IL-1 family of cytokines and localizes to the cell nucleus (Carriere et al., 2007; Cayrol and Girard, 2018; Schmitz et al., 2005). IL-33 is considered an alarmin since it lacks a signal peptide or other cellular export sequences, and is predominantly released into the extracellular space during necrotic or necroptotic cell death (Moussion et al., 2008). It is constitutively expressed in specialized subsets of epithelial cells, endothelial cells, and stromal cells in lymphoid and nonlymphoid tissues and in oligodendrocytes, astrocytes, and neurons in the CNS (Bonilla et al., 2012; Pichery et al., 2012).

IL-33 has been suggested to serve as an essential driver of local tissue accumulation of nonlymphoid tissue–residing T reg cells, which has been characterized best in the visceral adipose tissue (VAT) of male mice (Feuerer et al., 2009; Kolodin et al., 2015; Li et al., 2018; Vasanthakumar et al., 2020). The dominant

¹Howard Hughes Medical Institute and Immunology Program at Sloan Kettering Institute, New York, NY; ²Ludwig Center for Cancer Immunotherapy, Memorial Sloan-Kettering Cancer Center, New York, NY.

Correspondence to Saskia Hemmers: hemmers@mskcc.org; Alexander Y. Rudensky: rudenska@mskcc.org.

© 2020 Hemmers et al. This article is distributed under the terms of an Attribution–Noncommercial–Share Alike–No Mirror Sites license for the first six months after the publication date (see <http://www.rupress.org/terms/>). After six months it is available under a Creative Commons License (Attribution–Noncommercial–Share Alike 4.0 International license, as described at <https://creativecommons.org/licenses/by-nc-sa/4.0/>).

sources of IL-33 in adipose tissue are mesenchymal-derived stromal cells that are required to maintain immune cell homeostasis in lean mice (Mahlkōiv et al., 2019; Spallanzani et al., 2019). Adipose tissue T reg cells accumulate with age and express a characteristic transcriptional signature including *Il1rl1*, *Gata3*, *Klrg1*, and *Ili10* (Feuerer et al., 2009; Kolodin et al., 2015). This unique phenotype is dependent on expression of the nuclear receptor family member PPAR γ (Bapat et al., 2015; Cipolletta et al., 2012; Vasanthakumar et al., 2020). Loss of IL-33 or ST2 leads to a perturbation in the adipose tissue immune cell compartment, including a failure to maintain adipose tissue T reg cells, and manifests in increased weight gain and insulin resistance (Brestoff et al., 2015; Miller et al., 2010; Vasanthakumar et al., 2015). In addition, systemic delivery of recombinant IL-33 can potently drive proliferation of T reg cells and expand the pool of ST2⁺ T reg cells in an acute manner and has shown therapeutic benefits in mouse models of obesity (Han et al., 2015; Miller et al., 2010; Turnquist et al., 2011; Vasanthakumar et al., 2015). Whether IL-33/ST2 signaling promotes expansion of adipose tissue T reg cells in a cell-intrinsic or cell-extrinsic manner is a matter of contention. Besides direct signaling through the ST2 receptor expressed by T reg cells, various cell-extrinsic mechanisms have been proposed, including IL-33-dependent provision of IL-2 by dendritic cells (Matta et al., 2014) or mast cells (Morita et al., 2015) and inducible T cell costimulator ligand (ICOSL)-mediated expansion of adipose tissue T reg cells by type 2 innate lymphoid cells (ILC2s; Molofsky et al., 2015).

Thus, we sought to explore the cell-intrinsic requirements for ST2 expression by T reg cells using a novel conditional knockout (KO) allele of *Il1rl1*, the gene encoding ST2. We observed that ST2 expression was largely dispensable for T reg cell accumulation and maintenance in tissues at steady state and for IL-33-mediated expansion of T reg cells. The IL-33/ST2 signaling axis was, however, required to promote type 2 cytokine production by adipose tissue T reg cells. We also identified a novel role for T reg cells in limiting the size of the $\gamma\delta$ T cell population in an ST2-dependent manner in the CNS in a model of neuroinflammation, experimental autoimmune encephalomyelitis (EAE). Finally, we observed that the loss of ST2 on T reg cells resulted in disease exacerbation in EAE.

Results and discussion

Expression of ST2 is dispensable for the maintenance of tissue T reg cells at steady state

The receptor for IL-33, ST2, is prominently expressed on tissue T reg cells, especially in VAT. Mice that lack expression of either IL-33 or ST2 have a severe reduction in adipose tissue T reg cells and present with metabolic abnormalities, which are exacerbated in a model of high-fat diet-induced obesity (Vasanthakumar et al., 2015). Whether the reported dependence of tissue T reg cells on ST2 was a consequence of a cell-intrinsic requirement for ST2 on T reg cells has remained a contentious issue, especially considering the complex regulation of IL-33 signaling and its effects on multiple cell types and organismal physiology in general.

Therefore, we generated a novel conditional KO allele for *Il1rl1*, by genetically targeting exon 3 of the *Il1rl1* gene locus (Fig. S1 A). To confirm that deletion of our novel *Il1rl1* allele captures some previously described T reg cell-unrelated aspects of ST2 biology, we infected *Il1rl1*^{CD4cre} mice with lymphocytic choriomeningitis virus (LCMV). A previous study using mixed bone marrow chimeras and adoptive CD8 T cell transfers reported an essential cell-intrinsic role for ST2 signaling in protective CD8 T cell responses to LCMV infection (Bonilla et al., 2012). Our analysis of infected *Il1rl1*^{CD4cre} and littermate control mice confirmed the striking cell-intrinsic dependence on IL-33 signaling, whose disruption in virus-specific ST2-deficient CD8 T cells blunted their response to barely detectable levels (Fig. S1, B–F).

To explore a role for cell-intrinsic expression of ST2 in T reg cells, we ablated ST2 selectively in the T reg cell lineage by generating *Il1rl1*^{fl/fl}/*Foxp3*^{yfpcre} mice (Fig. 1 A). We found that while highly efficient, deletion of ST2 on T reg cells did not result in any measurable reduction of T reg cells in various lymphoid and nonlymphoid tissues analyzed (Fig. 1 B and Fig. S2 A). Moreover, T reg cells in epididymal white adipose tissue (eWAT) and skin maintained their characteristic expression of high levels of GATA3, KLRG1, and CD25 (Fig. 1 C). This disconnect with the severe reduction of adipose tissue T reg cells reported in germline ST2-deficient mice suggested that these effects are mostly driven in a T reg cell-extrinsic manner. It is possible that the adipose tissue T reg cell compartment is maintained by ILC2s, another cell type that is abundant in VAT, expresses high levels of ST2, and robustly expands in response to IL-33 (Molofsky et al., 2015). Similarly to studies in unchallenged mice, our analysis of potential effects of ST2 deficiency in T reg cells on a variety of infectious and inflammatory challenges, including influenza, LCMV Armstrong, and clone 13 virus infections, *Nippostrongylus brasiliensis* infection, bleomycin-induced lung injury, and 1-fluoro-2,4-dinitrobenzene-mediated delayed type hypersensitivity, failed to reveal any defect in accumulation or maintenance of ST2-deficient T reg cells in comparison to their ST2-sufficient counterparts (data not depicted).

It was also possible that the observed lack of functional consequences of ST2 ablation in T reg cells could simply be a reflection of the lack of access of ST2-expressing T reg cells to IL-33 rather than of redundancy of a role for direct IL-33 signaling in T reg cell residency in tissues with documented prominent IL-33 expression. T reg cells progressively accumulate in the VAT, with their numbers approaching a plateau by 5–7 mo of age (Feuerer et al., 2009; Kolodin et al., 2015). Gene expression analyses have revealed high expression of *Klrg1*, *Il1rl1*, *Gata3*, and *Ili10* (Feuerer et al., 2009; Vasanthakumar et al., 2020). Notably, GATA3-dependent expression of ST2 is a shared feature of T helper 2 (Th2) and T reg cells (Guo et al., 2009; Schiering et al., 2014). Stimulation of the former with IL-33 increases production of IL-5 and IL-13, which is independent of GATA3, but dependent on MAPK and NF- κ B signaling (Guo et al., 2009; Kurowska-Stolarska et al., 2008; Schmitz et al., 2005). Recently, it has been suggested that IL-33 might promote IL-5 and IL-13 secretion by ST2-expressing T reg cells in vitro and upon lung injury or allergen exposure (Chen et al., 2017; Liu et al., 2019; Siede et al., 2016). Because VAT T reg cells express high levels of ST2 and

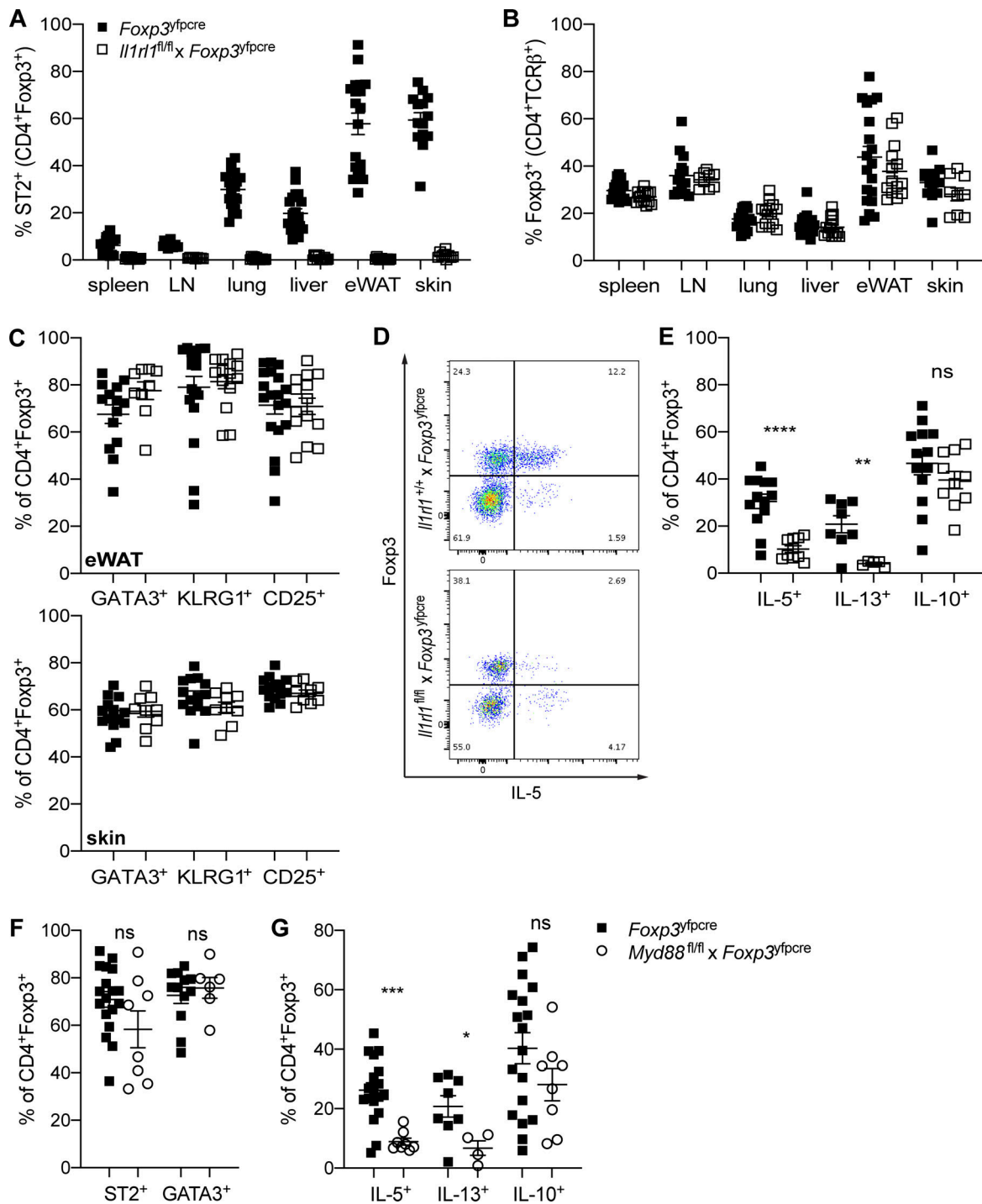


Figure 1. IL-33 signaling is not required to maintain tissue T reg cells but promotes type 2 cytokine production in adipose tissue. (A and B) Frequency of ST2-expressing T reg cells (A) or Foxp3-expressing cells among CD4⁺TCR β ⁺ cells (B) in lymphoid and nonlymphoid tissues of *Foxp3^{yfpcre}* ($n = 19$; black squares) or *Il1rl1^{fl/fl} × Foxp3^{yfpcre}* mice ($n = 9-14$; open squares). **(C)** Frequency of GATA3-, KLRG1-, or CD25-expressing T reg cells in eWAT (upper panel) or skin (lower panel) in *Foxp3^{yfpcre}* ($n = 14-19$; black squares) or *Il1rl1^{fl/fl} × Foxp3^{yfpcre}* mice ($n = 9-14$; open squares). **(D)** Representative example of intracellular cytokine staining for IL-5 after ex vivo stimulation with PMA and ionomycin (upper panel: *Foxp3^{yfpcre}*; lower panel: *Il1rl1^{fl/fl} × Foxp3^{yfpcre}*). **(E)** Quantification of IL-5-, IL-13-, and IL-10-expressing T reg cells in eWAT (as in D) contrasting *Foxp3^{yfpcre}* ($n = 8-13$; black squares) with *Il1rl1^{fl/fl} × Foxp3^{yfpcre}* mice ($n = 5-10$; open squares). IL-13 production was quantified in two independent experiments, whereas IL-5 and IL-10 production was assessed in all four experiments. **(F)** Frequency of ST2- or GATA3-expressing T reg cells in eWAT of *Foxp3^{yfpcre}* ($n = 12-18$; black squares) or *Myd88^{fl/fl} × Foxp3^{yfpcre}* mice ($n = 6-8$; open circles). **(G)** Quantification of IL-5-, IL-13-, and IL-10-expressing T reg cells in eWAT (as in D) contrasting *Foxp3^{yfpcre}* ($n = 8-18$; black squares) with *Myd88^{fl/fl} × Foxp3^{yfpcre}* mice ($n = 4-8$; open circles). All data were collected from 11-13-mo-old male mice. Data in A-C and E-G are plotted as means \pm SEM and are pooled from two to four independent experiments. ****, $P \leq 0.0001$; ***, $P \leq 0.001$; **, $P \leq 0.01$; *, $P \leq 0.05$; ns, $P > 0.05$ by unpaired t test.

reside in an IL-33-rich environment, we sought to ascertain that ST2 expression does impact functionality of VAT T reg cells by assessing type 2 cytokine secretion by this subset. Indeed, we readily detected IL-5 and IL-13 expression at the protein level upon ex vivo restimulation. This potential to secrete type 2 cytokines was strongly impaired in adipose tissue T reg cells lacking ST2 expression (Fig. 1, D and E). In contrast, secretion of IL-10 was unchanged. Signaling through the ST2 receptor requires the signaling adaptor MyD88. Indeed, *Myd88^{fl/fl}Foxp3^{yfpcre}* mice also displayed an impaired capacity to produce IL-5 and IL-13 despite normal expression levels of ST2 and GATA3 (Fig. 1, F and G). Altogether, this strongly suggested that cell-intrinsic IL-33 signaling, while promoting IL-5 and IL-13 secretion by adipose tissue T reg cells, is fully dispensable for their maintenance at steady state.

IL-33 efficiently drives T reg cell expansion independently of ST2 expression

Our observations that ST2 deficiency has no effect on accumulation of T reg cells residing in nonlymphoid organs including VAT and skin under physiological conditions was in contrast to the widely accepted view of an essential role for ST2 in maintenance and expansion of tissue T reg cells put forward by a number of previous reports (Li et al., 2018; Schiering et al., 2014; Vasanthakumar et al., 2015). This seeming discrepancy suggests that maintenance of tissue T reg cells is largely independent of cell-intrinsic expression of ST2 in unchallenged mice but is likely driven by cell-extrinsic IL-33/ST2 signaling. Thus, we set out to revisit the ability of systemically administered recombinant IL-33 to cause T reg cell expansion, previously considered by numerous studies as evidence of direct ST2-mediated signaling, by assessing a role for ST2 expression by T reg cells in this process (Fig. 2 A). Indeed, in agreement with previous reports, we observed that systemic delivery of IL-33 led to an efficient expansion of the T reg cell population in spleen, lung, and adipose tissue (Fig. 2, B and C; black squares versus blue squares). However, this effect was equally pronounced when T reg cells genetically lacked expression of ST2 (Fig. 2, B and C; blue filled versus open squares), suggesting that this expansion of T reg cells is driven by an intermediary cell type. Although the population size of ST2-sufficient and -deficient T reg cells was similarly affected, delivery of recombinant IL-33 promoted ST2 expression, as reflected by the increased proportion of ST2-expressing T reg cells, and also further augmented KLRG1 expression levels in the former, which was diminished in cells that genetically lacked expression of ST2 (Fig. 2, D–F). Expansion of GATA3-expressing T reg cells in the adipose tissue upon IL-33 treatment or expression of GATA3 or FOXP3 in those cells was unchanged (Fig. 2, E and F). When we analyzed production of IL-5 by T reg cells, we could detect a slight increase upon delivery of IL-33 in vivo, which trended lower in cells deficient for ST2 expression (Fig. 2 E), consistent with our observations in adipose tissue T reg cells (Fig. 1, D and E). Importantly, expansion of ILC2s, a subset of innate lymphoid cells that express high levels of ST2, was comparable between experimental groups (Fig. 2, G and H). Furthermore, these experiments provided additional support to ST2 deficiency being limited to the T reg cell lineage,

since expansion of CD4⁺Foxp3⁺ST2⁺ cells was not impaired in comparison to the control group (Fig. 2 H and Fig. S2 B). These results further support the notion that ST2 signaling in T reg cells has a notable impact on their activation and differentiation state yet is dispensable for the in vivo expansion and maintenance of T reg cells residing in secondary lymphoid organs and nonlymphoid tissues.

ST2-expressing T reg cells limit accumulation of $\gamma\delta$ T cells in VAT

Germline ST2- and IL-33-deficient mice present with metabolic abnormalities, including enhanced weight gain and defects in glucose metabolism (Brestoff et al., 2015; Miller et al., 2010; Vasanthakumar et al., 2015). In contrast, mice with a T reg cell-specific loss of ST2 exhibited slightly reduced body weight, adipose tissue weight, and liver weight in mice >45 wk of age (Fig. 3, A–C). The reduced adipose tissue size was mirrored by an overall reduction in immune cell numbers (Fig. 3 D), which was also observed in mice that lacked the essential ST2 signaling adaptor MyD88 (Fig. S2, C–F). The observed reduction in body weight and size of the adipose tissue compartment did not affect glucose tolerance in these animals (Fig. 3 H). Moreover, when mice with an ST2-sufficient or -deficient T reg cell compartment were fed a high-fat diet for 13 wk, weight gain and increase in adiposity and the size of the T reg compartment were indistinguishable between the two experimental groups (Fig. 3, I–K). This again is in stark contrast to what has been previously reported for ST2 KO mice, which gain more weight upon high-fat diet challenge and have impaired glucose tolerance (Miller et al., 2010).

Interestingly, upon a more careful analysis of the composition of the visceral adipose immune cell compartment, we detected a robust proportional increase of $\gamma\delta$ T cells (Fig. 3, E and F). Despite the reduction in overall immune cell content of the eWAT (Fig. 3 D), which was also reflected in the reduced numbers of CD4⁺ T cells and T reg cells, $\gamma\delta$ T cell numbers remained unchanged (Fig. 3 G). Importantly, the reduction of CD4⁺ T cells and T reg cells scaled with the reduction of overall immune cell numbers in the adipose tissue and was not observed in any other tissue analyzed (Fig. S2 G). The proportional increase of $\gamma\delta$ T cells is intriguing, since $\gamma\delta$ T cells have been implicated in the indirect regulation of the size of the T reg cell pool in adipose tissue (Kohlgruber et al., 2018) and in the neonatal lung during influenza infection (Guo et al., 2018). In both settings, production of IL-17A by $\gamma\delta$ T cells was shown to increase IL-33 production in the respective tissue, which then in turn promotes local expansion of T reg cells. Whether and how T reg cells reciprocally regulate the size of the $\gamma\delta$ T cell compartment in an ST2-dependent manner will be an interesting avenue for further investigation.

T reg cell-specific ST2 deficiency results in disease exacerbation in EAE

The observation that in physiological settings direct sensing of IL-33 by T reg cells affected their functionality (type 2 cytokine production and adipose tissue composition), we sought to assess a role for ST2 expression by T reg cells in an autoimmune

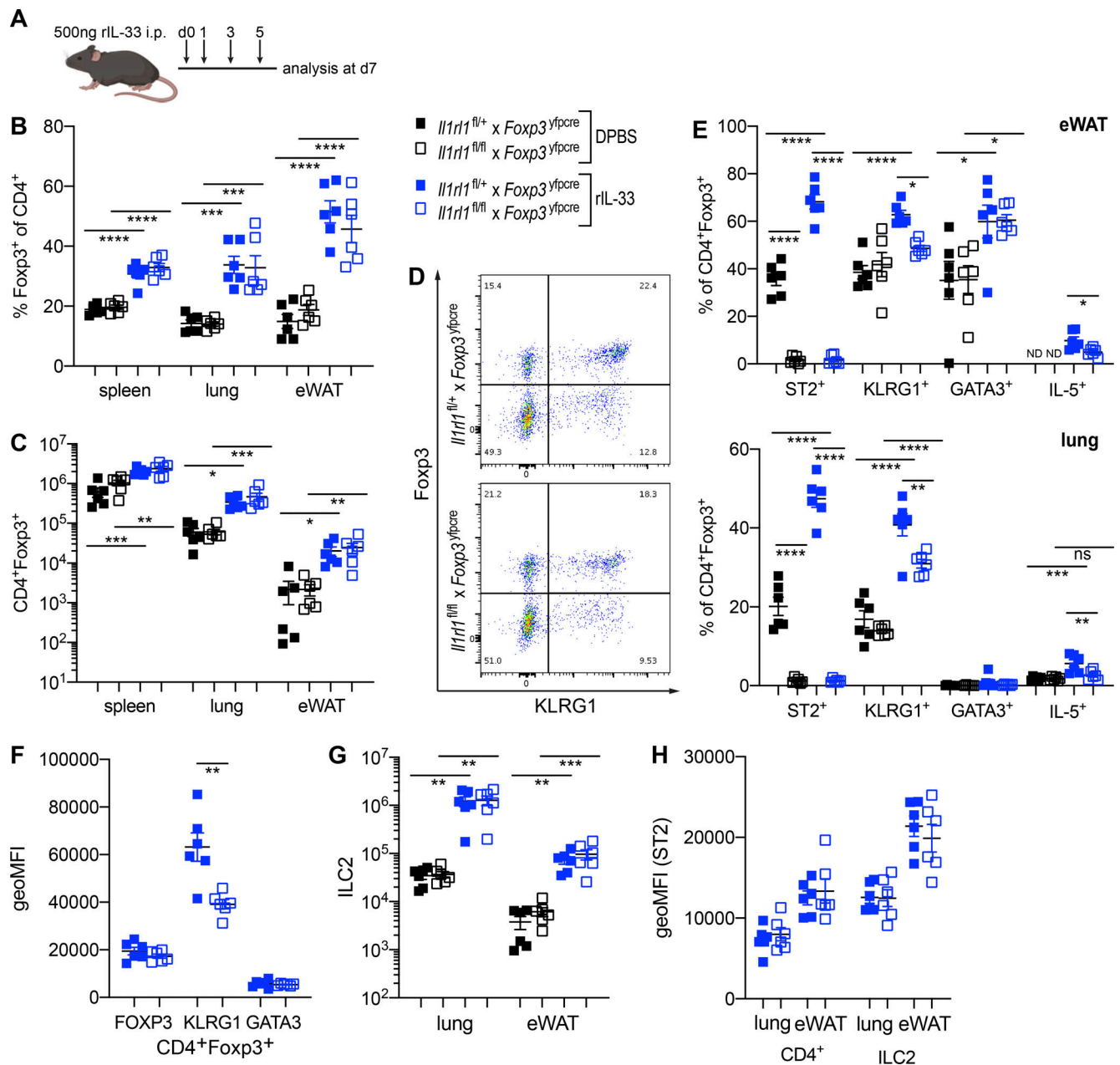


Figure 2. Systemic delivery of IL-33 drives T reg cell expansion independent of ST2 expression. (A) Mice received either DPBS or 500 ng of recombinant mouse IL-33 i.p. as indicated. (B and C) Frequency of Foxp3-expressing cells of CD4⁺ cells (B) or absolute numbers of T reg cells (C) in lymphoid and non-lymphoid tissues of *Il1rl1^{fl/fl} x Foxp3^{yfpcre}* (*n* = 6; DPBS, black filled squares; IL-33, black open squares) or *Il1rl1^{fl/fl} x Foxp3^{yfpcre}* mice (*n* = 6; DPBS, blue filled squares; IL-33, blue open squares). (D) Representative example of KLRG1 expression on the cell surface of CD4⁺TCRβ⁺ cells (upper panel: *Il1rl1^{fl/fl} x Foxp3^{yfpcre}*; lower panel: *Il1rl1^{fl/fl} x Foxp3^{yfpcre}*). (E) Frequency of ST2-, KLRG1-, GATA3-, or IL-5-expressing T reg cells in eWAT (upper panel) or lung (lower panel) contrasting *Il1rl1^{fl/fl} x Foxp3^{yfpcre}* (*n* = 6; DPBS, black filled squares; IL-33, black open squares) and *Il1rl1^{fl/fl} x Foxp3^{yfpcre}* mice (*n* = 6; DPBS, blue filled squares; IL-33, blue open squares). (F) Protein expression levels of FOXP3, KLRG1, and GATA3 on adipose tissue T reg cells from IL-33-treated mice are plotted for individual mice. (G) Total numbers of ILC2s (CD90⁺CD3ε⁻ST2⁺KLRG1⁺) are plotted for individual mice from lung and eWAT. (H) Protein expression levels of ST2 on lung and adipose tissue CD4⁺Foxp3⁻ T cells and ILC2s from IL-33-treated mice are presented. Data in B, C, and E–H are plotted as means ± SEM and are pooled from two independent experiments. ****, *P* ≤ 0.0001; ***, *P* ≤ 0.001; **, *P* ≤ 0.01; *, *P* ≤ 0.05 by one-way ANOVA with Sidak's multiple comparisons correction (B, C, E, and G) or unpaired *t* test (F and H). For clarity, only comparisons that were significantly different are indicated. ND, nondetectable; geoMFI, geometric mean fluorescence intensity.

inflammatory disease. IL-33 is highly expressed in myelinated areas of the brain and spinal cord, especially in brain endothelial cells, astrocytes, oligodendrocytes, and neurons (Fairlie-Clarke et al., 2018; Gadani et al., 2015; Jiang et al., 2012; Yasuoka et al.,

2011). We therefore reasoned that in EAE, a mouse model of neuroinflammation with features of immune-mediated tissue damage and a pathogenic T cell response, the IL-33/ST2 signaling axis might play an important role (Fig. S3, A and B). Indeed,

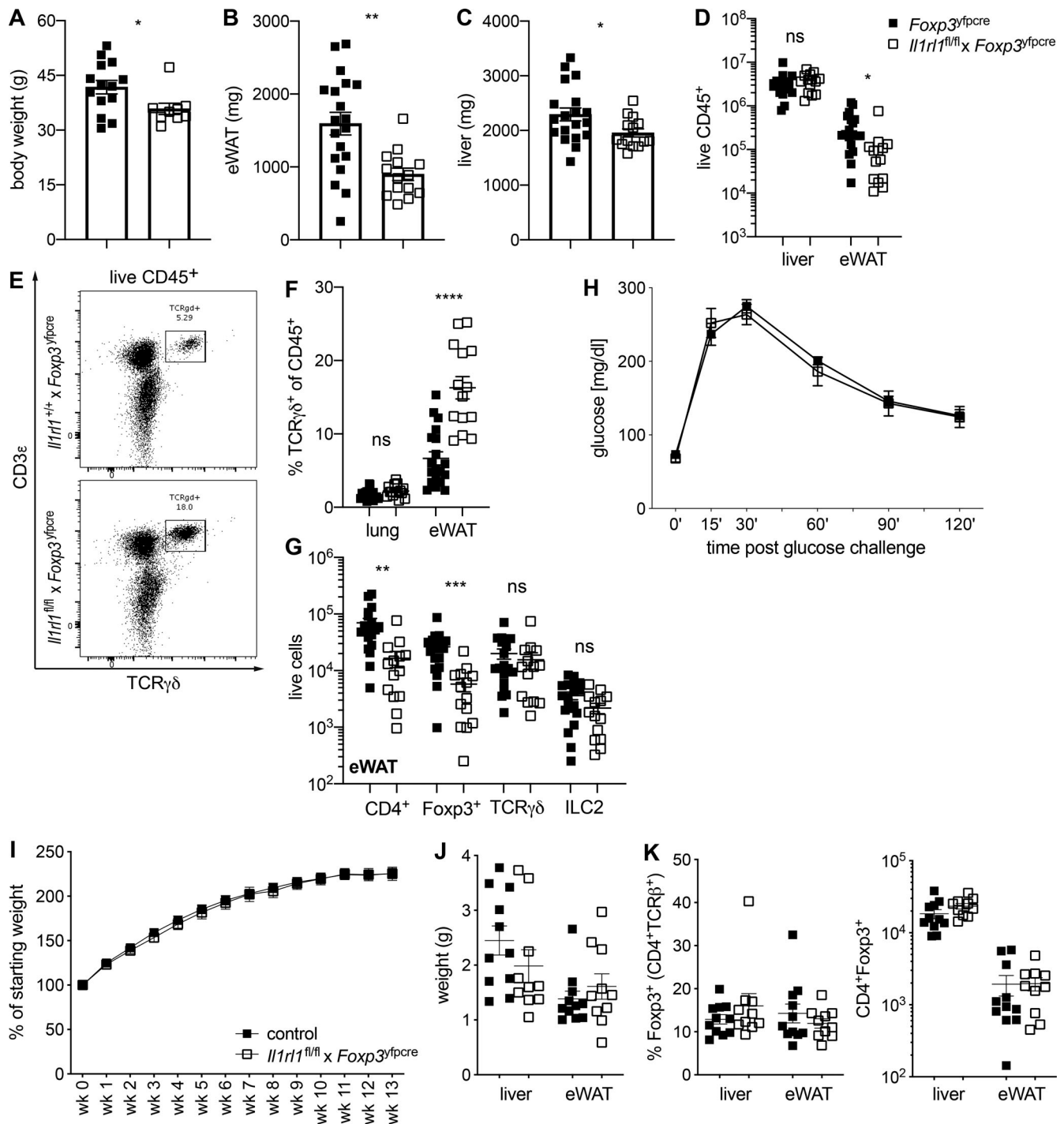


Figure 3. ST2-expressing T reg cells limit accumulation of $\gamma\delta$ T cells in VAT. (A–G) All data were collected from 11–13-mo-old male mice. (A–C) Total body weight (A), eWAT weight (B), and liver weight (C) are plotted for individual mice. (D) Quantification of immune cells in liver and eWAT of indicated mice. (E) Typical gating strategy to identify $\gamma\delta$ T cells (as CD3 ϵ ⁺TCR $\gamma\delta$ ⁺ cells of live CD45⁺ cells) in eWAT of indicated mice. (F) Relative abundance of TCR $\gamma\delta$ ⁺ cells among all CD45-expressing cells from *Foxp3^{yfpcre}* ($n = 14$ –19; black squares) or *Il1rl1^{fl/fl} × Foxp3^{yfpcre}* mice ($n = 9$ –14; open squares). (G) Absolute numbers of CD4⁺ T cells, T reg cells, $\gamma\delta$ T cells, and ILC2s in eWAT are plotted. (H) Blood glucose levels over 120 min after glucose challenge in 8-mo-old mice comparing *Foxp3^{yfpcre}* ($n = 8$; black squares) with *Il1rl1^{fl/fl} × Foxp3^{yfpcre}* mice ($n = 6$; open squares). (I–K) 6-wk-old male mice were placed on a high-fat diet for 13 wk, contrasting control mice ($n = 11$; black squares) with *Il1rl1^{fl/fl} × Foxp3^{yfpcre}* mice ($n = 10$; open squares). Body weight was monitored over time and is presented as percentage of starting weight (I). Weight of liver and eWAT are plotted for individual mice after 13 wk of high-fat diet feeding (J). Relative abundance of T reg cells among CD4⁺TCR β ⁺ cells (left) and absolute numbers of T reg cells (right) in eWAT (K). Data in A–D and F–G are plotted as means \pm SEM. A–D, F, and G are pooled from three to four independent experiments. Data in H are representative of two independent experiments. Data in I–K are pooled from two independent experiments. ****, $P \leq 0.0001$; ***, $P \leq 0.001$; **, $P \leq 0.01$; *, $P \leq 0.05$; ns, $P > 0.05$ by unpaired t test.

previous EAE studies have reported disease exacerbation in ST2 or IL-33 KO mice or mice treated with IL-33-neutralizing antibodies (Chen et al., 2015; Jiang et al., 2012; Milovanovic et al., 2012; Xiao et al., 2018). However, treatment with recombinant IL-33 has been reported to have either detrimental effects (Li et al., 2012) or a protective role on disease severity (Jiang et al., 2012), suggesting a complex interplay between ST2-expressing cell types at various stages of the disease. Moreover, IL-33 has also been implicated in both promoting (Gadani et al., 2015) and inhibiting (Allan et al., 2016) myelination in the CNS. Thus, we first analyzed IL-33 expression levels in the spinal cord over the course of disease in C57BL/6 mice. IL-33 protein expression was elevated in spinal cords of symptomatic mice, whereas the *Il33* transcript level remained unchanged (Fig. S3, C and D). Considering the essential role T reg cells play in disease mitigation (Koutouros et al., 2014), we carefully characterized the CNS-infiltrating T reg cell population and observed accumulation of ST2-expressing T reg cells over time (Fig. S3 E). This led us to ask if IL-33 signaling might control local T reg cell accumulation or function upon recruitment to the CNS. We immunized *Il1rl1^{fl/fl}Foxp3^{yfpcre}* mice that harbored ST2-deficient T reg cells with MOG peptide to induce EAE and monitored disease severity over time. Disease was exacerbated compared with control mice (Fig. 4 A). Overall immune cell infiltration into the CNS was comparable between experimental groups (Fig. 4 B). The relative proportion and absolute numbers of T reg cells were even somewhat increased in mice that lacked ST2 expression on T reg cells (Fig. 4 C). These results suggested that in the CNS, cell-intrinsic ST2 signaling in T reg cells was also not required to promote their local expansion. Microglia represent the central node of neuroimmune interaction in the CNS. Improper activation has been associated with neurological dysfunction and neurodegenerative diseases, including Alzheimer's disease and multiple sclerosis (Scheiblich et al., 2020). Therefore, we chose to profile the microglial compartment as a readout for CNS-resident immune cells. We detected a total of 14 differentially expressed genes when comparing microglia isolated from *Foxp3^{yfpcre}* (WT) and *Il1rl1^{fl/fl}Foxp3^{yfpcre}* (KO) at day 10 after EAE induction (13 increased in KO, fold change [FC] ≥ 2 ; 1 decreased in KO, FC ≥ 2 ; Fig. 4 D). Despite the small number of genes, it is remarkable that several of the genes identified (*Ptdgs*, *S1pr3*, and *Ccl22*) have been implicated in promoting neuroinflammation. Blockade of *Ccl22* dampens disease severity in EAE without an effect on the effector T (T eff) cell response (Dogan et al., 2011). Microglial-derived prostaglandin D2 can promote astrogliosis and demyelination (Mohri et al., 2006). Modulation of *S1pr3* signaling suppresses pathogenic microglia and astrocyte activation and chronic progressive CNS inflammation in EAE (Rothhammer et al., 2017).

Because pathology in this model of neuroinflammation is driven by pathogenic CD4⁺ T cells, which are characterized by their potential to secrete IFN γ , IL-17A, and GM-CSF (El-Behi et al., 2011; Goverman, 2009), we quantified production of these cytokines. However, we were unable to detect differences between the experimental groups (Fig. 4 E). In addition, we isolated T eff cells from spleen or CNS of *Foxp3^{yfpcre}* (WT) and *Il1rl1^{fl/fl}Foxp3^{yfpcre}* (KO) at days 0, 5, and 10 after EAE induction

and transcriptionally profiled these populations by RNA sequencing (RNA-seq; Fig. S3 F). Clustering of resulting gene expression features using principal component analysis (PCA) showed clear separation based on tissue of origin (PC1) and disease state (PC2), but no separation based on genotype (Fig. S3 G). Overall, we detected very few differentially expressed genes in T eff cells, which was in line with our phenotypic characterization in vivo and suggested other cellular targets for ST2-dependent T reg cell-mediated disease modulation (Fig. S3 H; some data not depicted).

We did, however, detect an increase in $\gamma\delta$ T cells infiltrating the CNS in the presence of ST2-deficient T reg cells (Fig. 4 F). These $\gamma\delta$ T cells produced more IL-17A and less IFN γ in the CNS and spleen compared with the control group of mice (Fig. 4, G and H; and data not depicted). A disease-promoting role for $\gamma\delta$ T cells in EAE has been established using *Tcrd^{KO}* mice and antibody-mediated depletion of $\gamma\delta$ T cells (Rajan et al., 1998; Spahn et al., 1999). This pathogenic role is associated with IL-17A-producing $\gamma\delta$ T cells ($\gamma\delta$ T17), the predominant subset within the CNS during peak of disease, whereas the IFN γ -producing subset has been associated with disease amelioration (Blink et al., 2014). $\gamma\delta$ T cells are one of the earliest sources of IL-17A within the CNS, since they have the ability to produce inflammatory mediators in response to IL-23 and IL-1 β (Sutton et al., 2009). This early response promotes the generation of pathogenic Th17 cells and is blunted in the absence of $\gamma\delta$ T cells (McGinley et al., 2020; Petermann et al., 2010). Interestingly, the peak of expansion of those $\gamma\delta$ T17 cells precedes the maximal expansion of T reg cells in the CNS, and *Tcrd^{KO}* mice have higher T reg cell frequencies and milder disease. This result suggested a crosstalk wherein $\gamma\delta$ T17 cells inhibit the T reg cell response to EAE, thereby enhancing disease (Petermann et al., 2010). Based on our data, we propose that T reg cells in turn also feed back on the size of the $\gamma\delta$ T17 cell population in an ST2-dependent manner, that this feedback control is important to promote recovery, and that lack thereof might at least in part contribute to disease exacerbation observed in our animal model (Fig. 4 A).

ST2-dependent transcriptional reprogramming of splenic T reg cells is most prominent early during EAE

To explore these novel ST2-dependent effects of T reg cells in more detail, we considered at least two nonmutually exclusive possibilities of interpreting the observed disease modulation: (1) the IL-33/ST2-axis drives a unique transcriptional program in T reg cells to promote disease amelioration and tissue repair; or (2) ST2 expression by T reg cells acts as a sink for IL-33, thereby reducing the bioavailability of IL-33 within the tissue. To address the first scenario, T reg cells were isolated from spleen or CNS of *Foxp3^{yfpcre}* (WT) and *Il1rl1^{fl/fl}Foxp3^{yfpcre}* (KO) at days 0, 5, and 10 after EAE induction and transcriptionally profiled by RNA-seq (Fig. S3 F).

Clustering of resulting gene expression features using PCA revealed a clear separation based on tissue of origin (PC1) and disease state (PC2; Fig. 5 A). We focused our analysis on the transcriptional profiles of T reg cells isolated from spleen at day 5, which showed a clear separation between WT and KO in the 3D PCA (Fig. 5 A; light green circles versus dark green circles)

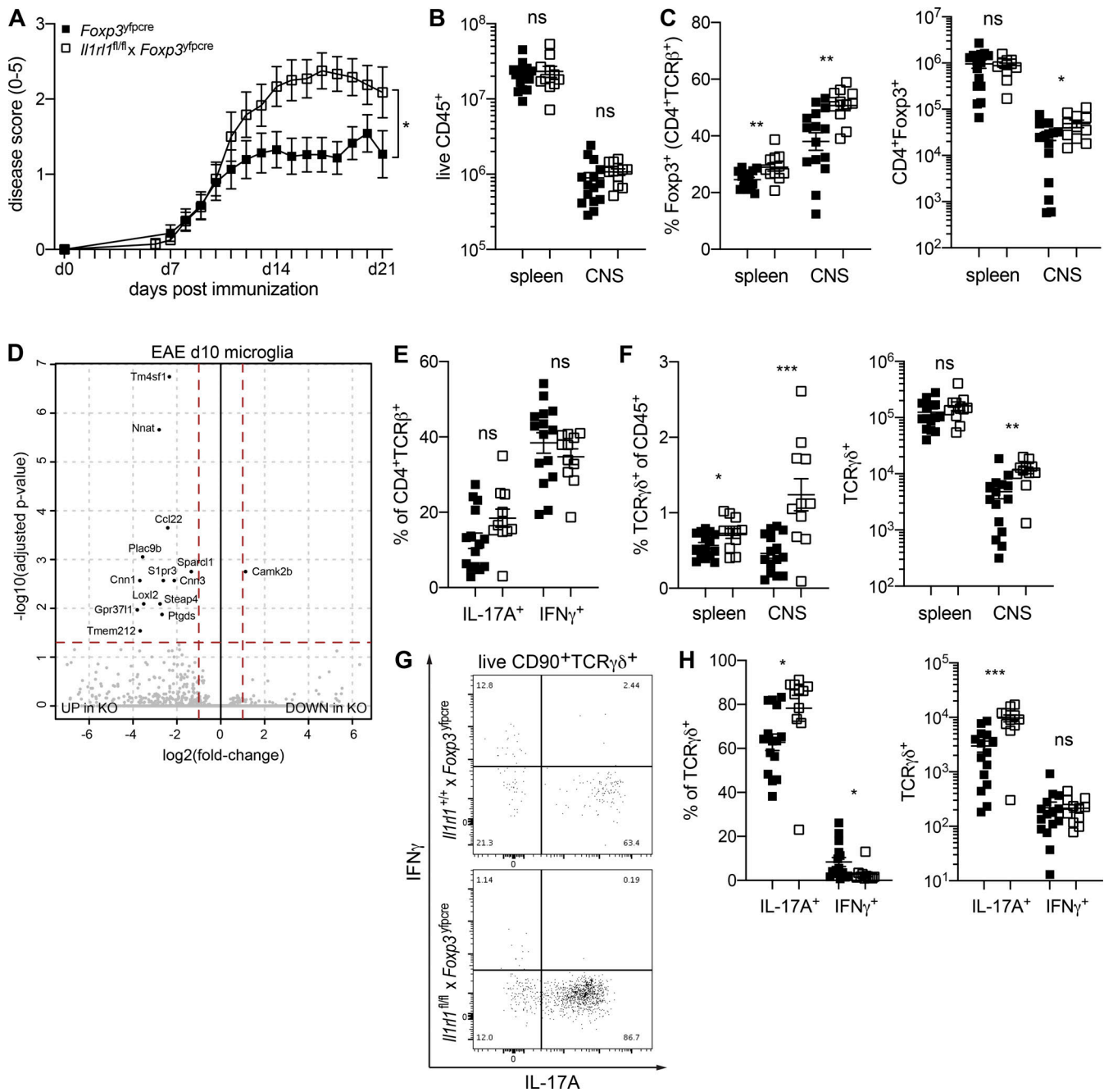


Figure 4. T reg cell-specific ST2 deficiency results in disease exacerbation in EAE. (A–C) 8–10-wk-old male mice were immunized with MOG/CFA to induce EAE. Disease was monitored daily starting at day 7 after immunization and is represented by a disease score plotted in A for *Foxp3^{yfpcre}* ($n = 23$; black squares) or *Il1r1^{fl/fl} × Foxp3^{yfpcre}* mice ($n = 24$; open squares). Total immune cells (B) and relative abundance (left) and total number of T reg cells (right; C) in spleen and CNS of *Foxp3^{yfpcre}* ($n = 15$; black squares) or *Il1r1^{fl/fl} × Foxp3^{yfpcre}* mice ($n = 11$; open squares) at day 21 after immunization. (D) Volcano plot of gene expression data contrasting microglia isolated from the CNS at day 10 after EAE induction from *Foxp3^{yfpcre}* (WT) or *Il1r1^{fl/fl} × Foxp3^{yfpcre}* (KO) mice. Genes with a FC ≥ 2 and an adjusted P value < 0.05 are labeled. Genes increased in KO are on the left; genes decreased in KO are on the right of the plot. (E) Assessment of IL-17A and IFN γ production after ex vivo stimulation with PMA and ionomycin by CD4⁺ T cells infiltrating the CNS. (F) Relative abundance (left) and total number (right) of $\gamma\delta$ T cells in spleen and CNS day 21 after disease induction. (G) Assessment of IL-17A and IFN γ production after ex vivo stimulation with PMA and ionomycin by TCR $\gamma\delta$ ⁺ cells in the CNS by flow cytometry. Cells were pregated on live CD90⁺TCR $\gamma\delta$ ⁺ cells. (H) Data from G plotted for individual mice as frequency of cytokine producers (left) and total number of cytokine-producing $\gamma\delta$ T cells in the CNS. Data in A–C, E, F, and H are plotted as means \pm SEM and pooled from four (A) and two (all others) independent experiments. ***, $P \leq 0.001$; **, $P \leq 0.01$; *, $P \leq 0.05$; ns, $P > 0.05$ by unpaired t test (B, C, E, F, and H). Statistical significance in A was assessed by comparison of the area under the curve for individual mice using the nonparametric unpaired two-tailed Mann–Whitney U test.

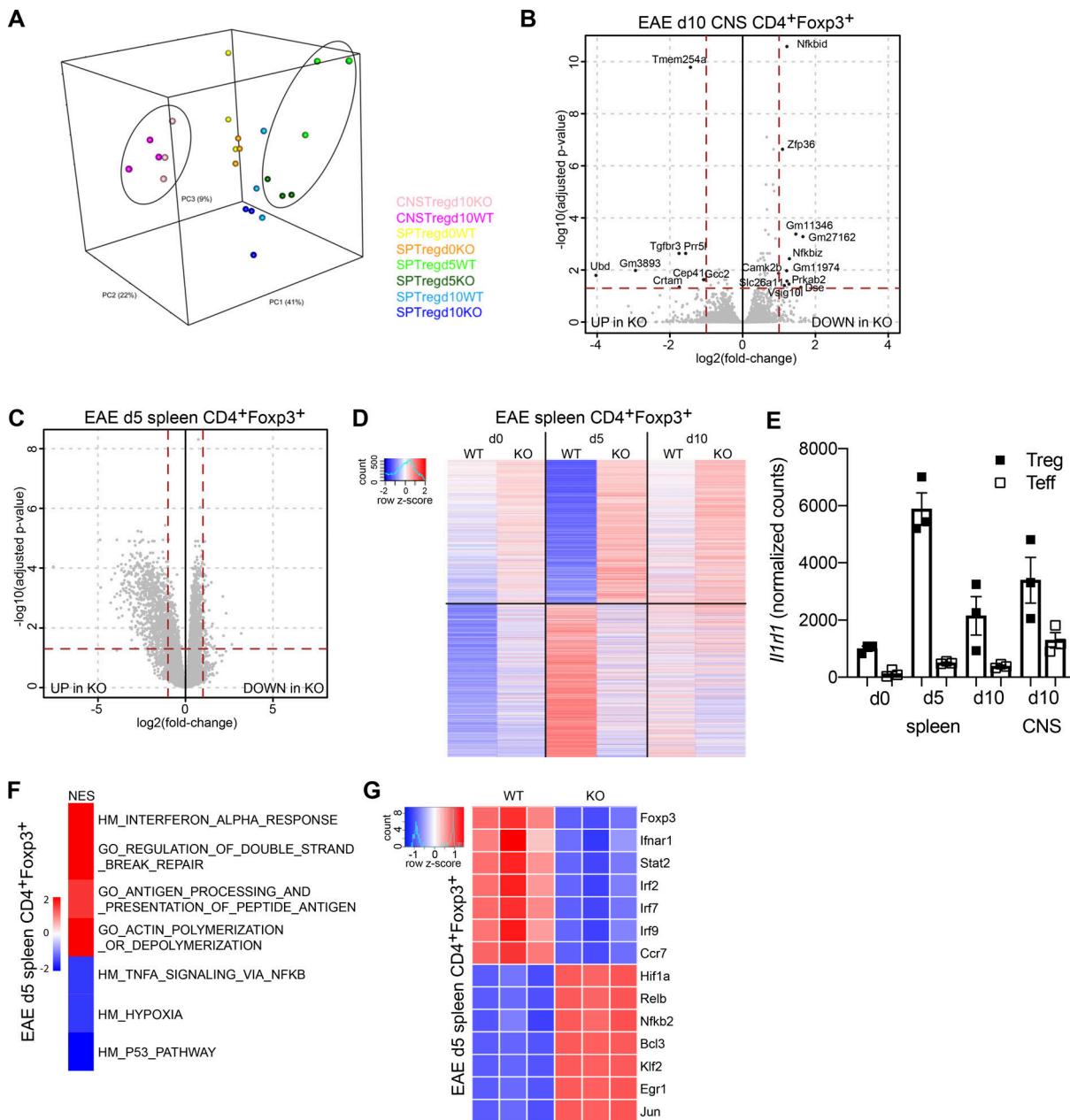


Figure 5. ST2-dependent transcriptional reprogramming of splenic T reg cells is most prominent early during EAE. (A) 3D PCA of T reg cells from spleen (days 0, 5, and 10) and CNS (day 10). **(B and C)** Volcano plot of gene expression data contrasting T reg cells isolated from the CNS at day 10 (B) or spleen at day 5 (C) after EAE induction from *Foxp3^{fl/cre}* (WT) or *Il1r1^{fl/fl} × Foxp3^{fl/cre}* (KO) mice. Genes with a FC ≥ 2 and an adjusted P value < 0.05 are labeled (B). Genes increased in KO are on the left; genes decreased in KO are on the right of the plot. **(D)** Relative average gene expression of a defined gene set (genes differentially expressed between T reg cells isolated from spleen at day 5) of splenic T reg cells at days 0, 5, and 10 after EAE induction. **(E)** Normalized *Il1r1* transcript levels extracted from RNA-seq analysis in T reg cells and CD4 T eff cells in spleen and CNS at various time points after EAE induction. **(F)** Pathways enriched among differentially expressed genes in T reg cells isolated from spleen at day 5 after EAE induction. Only pathways with a false discovery rate $< 25\%$ are shown, and the normalized enrichment score (NES) is visually represented. **(G)** Normalized expression of selected differentially expressed genes comparing WT and KO T reg cells isolated from spleen at day 5 after EAE induction. PC, principal component.

and cells isolated from the CNS at day 10 (Fig. 5 A; light pink circles versus dark pink circles). We identified a total of 64 differentially expressed genes, 21 of which exhibited a FC of ≥ 2 between the CNS samples (16 increased in KO, 8/16 with FC ≥ 2 ; 48 decreased in KO, 13/48 with FC ≥ 2 ; Fig. 5 B). Overall, there were no changes in expression of genes associated with T reg cell maintenance or suppressive capacity. Interestingly, the genes

that were expressed at lower levels within the ST2-deficient T reg cells included targets of NF- κ B signaling (*Nfkbia*, *Nfkbid*, *Nfkbiz*, *Cd69*, *Trafi1*, and *Zfp36*). This suggested that T reg cells within the CNS experience active IL-33/ST2/MyD88 signaling that was diminished in the absence of the receptor. Because ST2-expressing T reg cells represent only a fraction (~20%) of T reg cells within the CNS at day 10 after EAE induction, and we

observed very limited changes in gene expression, it is difficult to pinpoint potential novel function-related molecules within this subset, offering a rationale for an in-depth molecular and functional dissection of the ST2-expressing subset of T reg cells residing in the CNS in future studies.

When we assessed gene expression changes in splenic T reg cells isolated at day 5 after EAE induction, we discovered a large number of differentially expressed genes (1,345 increased in KO, 930/1,345 with $FC \geq 2$; 1,405 decreased in KO, 52/1,405 with $FC \geq 2$; Fig. 5 C). We used the newly discovered set of differentially expressed genes and compared it to the average gene expression in splenic T reg samples from days 0 and 10 after EAE induction (Fig. 5 D). The genes that were up-regulated in KO cells at day 5 showed similar trends in the day 0 and 10 comparisons (Fig. 5 D, upper half). The genes that were down-regulated in KO at day 5 might represent an inflammation-dependent module that is induced in WT T reg cells (going up from day 0 to 5) but does not display a similar behavior in KO T reg cells (Fig. 5 D, lower half). This suggested that this inflammation-dependent module was at least in part downstream of the IL-33/ST2 signaling axis.

It has been appreciated that local inflammation can promote transient induction of IL-33 in radioresistant cells of the splenic T cell zone. This local increase in IL-33 is essential for driving the antiviral T cell response during LCMV infection (Bonilla et al., 2012). We speculated that after immunization with MOG/CFA to induce EAE, local inflammation in the spleen might lead to transient induction of IL-33 that then in turn promotes the expansion of ST2-expressing T reg cells locally or induces de novo expression of ST2 on T reg cells. Indeed, when we quantified *Il1rl1* transcript levels in T reg cells, expression was highest in cells isolated from spleen at day 5 after EAE induction (Fig. 5 E). We performed gene set enrichment analysis to identify pathways that were specifically affected by the loss of ST2 on T reg cells at day 5 (Fig. 5 F). Biological processes that were under-represented in KO T reg cells included the type I IFN response, double-strand break repair, and cellular regulation of actin dynamics. Interestingly, *Ifnar1*, the gene encoding for a subunit of the type I IFN receptor, and *Stat2*, its downstream signal transducer, were among genes differentially expressed in T reg cells at day 5, with lower expression in ST2-deficient cells (Fig. 5 G). Pathways that were more engaged in T reg cells that genetically lacked ST2 included the p53 pathway, the response to hypoxia, and TNF α signaling via NF- κ B. In agreement with that, expression of *Hif1a*, the master regulator of the hypoxia response, was increased more than twofold in ST2-deficient T reg cells. In addition, the transcripts encoding NF- κ B family members RELB and NFKB2 were also expressed at higher levels in ST2-deficient T reg cells, potentially contributing to the enrichment in genes associated with the TNF α signaling via NF- κ B pathway, including the transcription factors *Klf2*, *Bcl3*, *Egr1*, and *Jun* (Fig. 5 G).

A role for ST2 expression on T reg cells has been mostly associated with their residence in nonlymphoid tissues, most prominently the adipose tissue, skin, and colon. Based on our RNA-seq data, we propose that ST2 signaling might also play an important role in the spleen in the context of a strong inflammatory response. The high transcript levels of *Il1rl1* in T reg cells

at day 5 after EAE induction suggest that the inflammatory environment might specifically expand ST2-expressing T reg cells or induce de novo expression of ST2 on T reg cells. ST2 expression on T reg cells was recently described to be a marker of the most mature tissue T reg precursors found in the spleen (Delacher et al., 2020). Our data suggest that lack of the ST2 receptor does not impede the expansion of T reg cells during EAE altogether, but rather changes the quality of the cells that expand, based on the large number of differentially expressed genes we detected in splenic T reg cells at day 5. If these cells are destined to seed tissues, as proposed by recent studies, inappropriate programming through a lack of signaling input via ST2 might have long-lasting consequences.

Concluding remarks

Our studies suggested that ST2 expression on T reg cells was largely dispensable for their accumulation and residence in tissues at steady state, in contrast to major defects in T reg cell accumulation, especially in adipose tissue and colon, caused by a germline ST2 deficiency (Kolodin et al., 2015; Schiering et al., 2014; Vasanthakumar et al., 2015) or the T reg cell-specific requirement for ST2 signaling to promote skeletal muscle repair (Kuswanto et al., 2016). Our observations cannot be simply explained by “ignorance,” i.e., insufficient access of T reg cells to IL-33, as cell-intrinsic ST2 signaling was required for type 2 cytokine secretion by VAT T reg cells. Additionally, we found that even though systemic provision of IL-33 was a powerful driver of T reg cell expansion in lymphoid and nonlymphoid tissues, comparable increases were observed in ST2-sufficient and -deficient T reg cells. These findings highlight the complex cell-extrinsic regulation of T reg cell tissue residence and accumulation promoted by a network of IL-33-responsive cell types, likely including ILC2s and mast cells (Molofsky et al., 2015; Morita et al., 2015).

Although VAT T reg population size was not affected by the absence of cell-intrinsic IL-33 signaling, it severely curtailed the ability of T reg cells to limit the size of the $\gamma\delta$ T cell population in the adipose tissue. Intriguingly, $\gamma\delta$ T cells have been implicated in the regulation of the size of the T reg cell pool in adipose tissue and lung via local production of IL-17A that in turn drives IL-33-dependent expansion of T reg cells (Guo et al., 2018; Kohlgruber et al., 2018). Our study provides evidence that T reg cells in turn can reciprocally regulate the size of the $\gamma\delta$ T cell compartment of the adipose tissue in an ST2-dependent manner. Moreover, this ST2-dependent control of the $\gamma\delta$ T cell population was not limited to the steady state but was also observed in the context of neuroinflammation. ST2-deficient T reg cells failed to effectively control the accumulation of pathogenic IL-17A-producing $\gamma\delta$ T cell ($\gamma\delta$ T17) cells during EAE challenge, which might at least in part contribute to the disease exacerbation observed in this mouse model.

Notably, disease exacerbation did not correlate with a failure to accumulate T reg cells in the CNS or an increased pathogenic CD4 T cell response. Furthermore, the worsened disease severity was unlikely due to diminished Areg production by local ST2-deficient T reg cells, since mice harboring Areg-deficient T reg cells showed EAE severity comparable to that of controls (data not depicted). However, the observed changes in the gene

expression profiles caused by ST2 loss, which were limited in T reg cells infiltrating the inflamed CNS but much more prominent in splenic T reg cells early during EAE induction, suggest a qualitative difference in the response. Splenic T reg cells expressed high levels of *Il1rl1* transcript at that time point, suggesting they might be especially sensitive to IL-33 in the environment. There is evidence that in certain infectious settings, specialized stromal cells within the spleen can express high levels of IL-33 (Bonilla et al., 2012). We speculate that in the inflammatory context of EAE induction, there might be a similar spike of bioactive extracellular IL-33 within the spleen. This transient provision of IL-33 could either expand a small population of T reg cells that express ST2 or could induce ST2 expression de novo on T reg cells in this inflammatory context, potentially in conjunction with TCR signaling in a spatiotemporally organized functional niche. These specialized niches might be preexisting and representative of compartmentalized T reg cell populations, in agreement with the recent discovery of nonlymphoid tissue precursors within spleen and lymph nodes (Delacher et al., 2020; Miragaia et al., 2019). Besides ST2, T reg cells express other IL1R family members, including IL18R and IL1RI. All three receptors signal through MyD88 and could theoretically drive redundant gene expression programs. Specialization could occur through nonredundant expression of the receptors themselves or through context-specific local delivery of the ligand. In this regard, the cell types that can provide IL-33 to T reg cells, including stromal cells, endothelial cells, and epithelial cells are likely different from sources of IL-18 or IL-1, predominantly produced by monocytes and dendritic cells in an inflammatory setting. These cellular sources provide the opportunity for a layered response in a spatiotemporal manner and might help to tailor T reg cell functionality, especially in inflammatory settings.

Materials and methods

Mice

Myd88^{fl} (B6.129P2(SJL)-*Myd88^{tm1Defr}/J*), *CD4^{cre}* (B6.Cg-Tg(Cd4-cre)1Cwi/Bfluj), and *Foxp3^{YFPcre}* (B6.129(Cg)-*Foxp3^{tm4(YFP/cre)Ayr}/J*) mice have been described previously (Hou et al., 2008; Lee et al., 2001; Rubtsov et al., 2008). *Foxp3^{YFPcre}* were maintained in-house, and the rest of the mice were obtained from the Jackson Laboratory.

Il1rl1^{fl} mice were generated as depicted in Fig. S1 A. A targeting vector construct containing floxed exon 3 of the *Il1rl1* gene was generated by PCR amplification and subsequent cloning into the *pRapidFlirt* vector (Hövelmeyer et al., 2007). Briefly, a 3-kb short arm, a 1-kb floxed exon 3 fragment, and a 5-kb long arm were amplified from bacterial artificial chromosome clone RP24-189E6. The fragments were cloned into the vector using NotI, SalI, and XhoI, respectively. B6-Albino embryonic stem cells were electroporated with the linearized targeting vector. Obtained clones were screened by Southern blot to confirm specific recombination and integration of the targeting vector, in which exon 3 of murine *Il1rl1* was flanked by *loxP* sites and an *frt*-flanked neomycin resistance (*neo*) cassette. Positive clones were injected into C57BL/6 blastocysts, and resulting chimeric

progeny were bred to confirm germline transmission. Excision of *neo* was obtained by breeding with flip-recombinase (FlpE) transgenic mice, resulting in germline-targeted *Il1rl1^{fl}*.

Il1rl1^{fl} mice were used to generate *Il1rl1^{CD4cre}* mice by breeding with B6.Cg-Tg(Cd4-cre)1Cwi/Bfluj mice, and *Il1rl1^{fl/fl}Foxp3^{YFPcre}* mice by breeding with B6.129(Cg)-*Foxp3^{tm4(YFP/cre)Ayr}/J* mice. *Myd88^{fl}* mice were bred to B6.129(Cg)-*Foxp3^{tm4(YFP/cre)Ayr}/J* mice to generate *Myd88^{fl/fl}Foxp3^{YFPcre}* mice.

All animals were maintained in the Memorial Sloan-Kettering Cancer Center animal facility under specific pathogen-free conditions, and experiments were performed according to institutional guidelines (institutional animal care and use committee 08-10-23). Studies were performed exclusively on male mice. Age of mice is specified in the figure legends. Mice were age-matched, and mice from the same litter were analyzed together whenever possible. Because our analysis is limited to male mice, performing experiments only with littermates is prohibitive, so age-matched mice from multiple breeding cages were analyzed together. All control mice came from the same breeding colony and the same strain background; nonrelated control mice from outside vendors were not used in this study.

To model diet-induced obesity, 6-wk-old male mice were placed continuously on a rodent diet with 60 kcal% fat (D12492; Research Diets). Weight gain was monitored by weighing the mice once per week over a period of 13 wk.

Tissue preparation and cell isolation

Spleen and lymph nodes were mechanically dissociated between frosted glass slides or with the back of a syringe plunger and filtered through a 100- μ m nylon mesh to yield single-cell suspensions. For analysis of immune cells from lung, liver, eWAT, and skin, tissues were isolated after pericardial perfusion with ice-cold Dulbecco's PBS (DPBS). Tissues were enzymatically digested in 4 ml of 1 mg/ml collagenase A from *Clostridium histolyticum* (Roche) and 1 U/ml DNaseI in RPMI 1640 with 2% FBS, 100 μ g/ml penicillin/streptomycin, 20 mM L-glutamine, and 10 mM Hepes (for eWAT, 30 min; lung/liver, 45 min; skin, 60–75 min) at 37°C while shaking in the presence of three 0.25-inch ceramic spheres (MP Biomedicals). Digested tissue was filtered through 100- μ m cell strainers and further cleaned up by 40% Percoll (GE Healthcare) centrifugation. Cells were resuspended in RPMI-10 (RPMI 1640, 10% FBS, 20 mM L-glutamine, 100 μ g/ml penicillin/streptomycin, 10 mM Hepes, 1 mM sodium pyruvate, 1 \times MEM nonessential amino acids, and 10⁻⁵ M 2-mercaptoethanol). To assess cytokine production ex vivo, single-cell suspensions were incubated for 3–4 h at 37°C with 5% CO₂ in the presence of 50 ng/ml PMA and 500 ng/ml ionomycin with 1 μ g/ml brefeldin A (all Sigma-Aldrich) and 2 μ M monensin (BioLegend). To analyze cytokine production in LCMV-infected mice, single-cell suspensions were stimulated for 5 h at 37°C with soluble anti-CD3 (5 μ g/ml; 2C11; BioXCell) and anti-CD28 (5 μ g/ml; 37.51; BioXCell) or specific peptides (described below; 1 μ g/ml) in the presence of 1 μ g/ml brefeldin A (Sigma-Aldrich) and 2 μ M monensin (BioLegend).

Flow cytometry and antibodies

All flow cytometry data were collected on an LSRII (BD) flow cytometer or the Aurora spectral analyzer (Cytex) and analyzed

using FlowJo 9 and 10 software (TreeStar). Single-cell suspensions were resuspended in DPBS and stained with Ghost Dye Violet 510 or Ghost Dye Red 780 (Tonbo) for dead-cell exclusion in the presence of anti-CD16/32 (Tonbo) to block binding to Fc receptors for 10 min at 4°C. Cell surface antigens were stained for 20 min at 4°C in FACS buffer (DPBS, 0.5% BSA [VWR], and 2 mM EDTA). Cells were analyzed unfixed, fixed with 2% paraformaldehyde (Thermo Fisher Scientific) for later analysis, or fixed and permeabilized with the BD Cytofix/Cytoperm kit (for intracellular cytokine staining) or the eBioscience Foxp3/Transcription Factor staining buffer set. Fixation, permeabilization, and intracellular staining were performed as recommended by the manufacturers. All cells were resuspended in FACS buffer and filtered through 100- μ m nylon mesh before analysis on the flow cytometer. 123count eBeads (eBioscience) were added at 5,000 beads per sample to quantify absolute cell numbers. Antibodies used in this study were purchased from BioLegend, BD Biosciences, eBioscience/Thermo Fisher Scientific or Tonbo Bioscience. The following clones were used: CD45 (30-F11), CD45.2 (104) NK1.1 (PK136), Ter-119 (Ter-119), TCR γ δ (GL3), TCR β (H57-597), CD3 ϵ (145-2C11), CD4 (RM4-5, GK1.5), CD8a (53-6.7), CD8b (YTS156.7.7), CD62L (MEL-14), CD44 (IM7), CD25 (PC61), CD90.2 (30-H12, 53-2.1), B220 (RA3-6B2), CD19 (6D5, 1D3), CD11b (M1/70), Siglec F (E50-2440), Klr g 1 (2F1), ST2 (DIH9), Gata3 (TWAJ), Foxp3 (FJK-16s), IFN γ (XMG1.2), IL-17A (TC11-18H10.1), IL-5 (17A2), IL-13 (eBio13A), and IL-10 (JES5-16E3).

LCMV infection

8-wk-old mice were infected i.p. with 2×10^5 PFU LCMV Armstrong and analyzed on day 7 after infection. Virus-specific T cells were quantified in spleen and liver with MHC class I tetramers of H-2D^b complexed with NP₃₉₆₋₄₀₄(FQPQNGQFI) or GP₃₃₋₄₁(KAVYNFATM), obtained from the National Institutes of Health tetramer core as monomers and tetramerized with PE-conjugated streptavidin (Molecular Probes) in-house. Antiviral T cell responses were monitored by measuring cytokine-producing cells after restimulation with virus-derived peptides (GP₃₃₋₄₁(KAVYNFATM), GP₂₇₆₋₂₈₆(SGVENPGGYCL), GP₆₁₋₈₀(GLK GPDYKGVYQFKSVEFD), NP₃₉₆₋₄₀₄(FQPQNGQFI), and NP₃₀₉₋₃₂₈(SGEGWPYIACRTSVVGRAW); GenScript).

IL-33 delivery in vivo

Male mice received either DPBS or 500 ng recombinant mouse IL-33 (carrier-free; BioLegend) i.p. for a total of four doses (days 0, 1, 3, and 5). Mice were analyzed on day 7 after treatment initiation (see also Fig. 2 A).

Glucose tolerance test

8-mo-old mice were fasted for 12 h overnight and injected with D-glucose (Sigma-Aldrich) at 2 g/kg i.p. The tip of the tail was nicked, and blood glucose was monitored using the Contour blood glucose meter and test strips (Bayer) at various time points after glucose challenge (0, 15, 30, 60, 90, and 120 min).

EAE mouse model

All experiments were performed with male mice 8–12 wk of age. EAE was induced by immunization with 100 μ g myelin

oligodendrocyte glycoprotein-derived peptide (MOG₃₅₋₅₅, MEVGVYRSRPFVSRVHLYRNGK; GenScript) emulsified in CFA (Sigma-Aldrich), and 200 μ g *Mycobacterium tuberculosis* H37 Ra (BD 231141) s.c., followed by two doses of 200 ng pertussis toxin (Millipore/EMD) i.p. on days 0 and 2 after immunization. Mice were monitored for signs of disease and assigned a disease score as previously described (Stromnes and Goverman, 2006). Animals were analyzed at time points as indicated.

All animals were perfused with 10–20 ml ice-cold DPBS before tissue harvest. Brain and spinal cords were dissected, placed in 5-ml tubes, and enzymatically digested with 2 mg/ml collagenase A from *C. histolyticum* (Roche) and 1 U/ml DNaseI in RPMI 1640 with 2% FBS, 100 μ g/ml penicillin/streptomycin, 20 mM L-glutamine, and 10 mM Hepes for 30–45 min at 37°C while shaking in the presence of three 0.25-inch ceramic spheres (MP Biomedicals). Digested tissue was filtered through 100- μ m cell strainers and further cleaned up with 40% Percoll (GE Healthcare) centrifugation. Cells were resuspended for further analysis in RPMI-10 (RPMI-1640, 10% FBS, 20 mM L-glutamine, 100 μ g/ml penicillin/streptomycin, 10 mM Hepes, 1 mM sodium pyruvate, $1 \times$ MEM nonessential amino acids, 10^{-5} M 2-mercaptoethanol).

IL-33 protein and mRNA levels were quantified in spinal cord homogenates collected over a time course as indicated in Fig. S3 A. For IL-33 protein quantification, a 1-cm piece of lumbar spinal cord was homogenized in 1 ml ice-cold DPBS with protease inhibitors (Pierce Halt Protease Inhibitor Cocktail with EDTA; Thermo Fisher Scientific) by bead beating for 30 s with a 0.25-inch ceramic sphere (MP Biomedicals). The homogenate was cleared of insoluble material by centrifugation, and the supernatant was transferred into a fresh tube and stored at -80°C until further processing. IL-33 protein was measured using the mouse IL-33 Ready-SET-Go! ELISA kit (eBioscience/Invitrogen) according to the manufacturer's instructions. ELISA plates were read at OD₄₅₀ on a Synergy HTX instrument (BioTek). IL-33 levels were calculated through extrapolation from a standard curve using Prism 7 software. The results were normalized to total protein content within the sample that had been quantified using the Pierce BCA Protein Assay Kit (Thermo Fisher Scientific).

IL-33 transcript was quantified by quantitative RT-PCR. Total RNA was prepared from a 1-cm piece of lumbar spinal cord homogenized in 1 ml TRIzol reagent (Life Technologies) by bead beating for 30 s with a 0.25-inch ceramic sphere (MP Biomedicals). The homogenate was cleared of insoluble material by centrifugation, and the supernatant was transferred into a fresh tube and stored at -80°C until further processing. RNA was extracted by mixing the precleared supernatant with 200 μ l chloroform (Sigma-Aldrich) using Phase Lock Gel Heavy 2-ml tubes (5Prime; Thermo Fisher Scientific) for phase separation. The aqueous phase was transferred into a fresh tube and mixed with an equal amount of 70% (vol/vol) ethanol (Sigma-Aldrich) and loaded onto an RNeasy mini spin column (RNeasy Mini kit; Qiagen). RNA was prepared following the instructions of the kit, and RNA concentration and quality were assessed using a Nanodrop instrument (Thermo Fisher Scientific). The RNA (1 μ g) was reverse transcribed into cDNA using the qScript cDNA SuperMix (Quanta Biosciences). Quantitative PCR was

performed on an ABI PRISM7700 cycler (Applied Biosystems) using Power SYBR Green PCR master mix (Applied Biosystems) with the following primers: *Il33*: forward, 5'-TCCAACCTCCAAGA TTTCCCG-3', and reverse, 5'-CATGCAGTAGACATGGCAGAA-3' (Liang et al., 2013); *Hprt*: forward, 5'-GCCCTTGACTATAATGAG TACTTCAGG-3', and reverse, 5'-TTCAACTTGGCTCATCTTAG G-3' (Sandler et al., 2003).

Statistical analysis

Graph Pad Prism (v7 and v8) was used for all statistical analysis for biological experiments. We calculated P values as indicated in the figure legends; differences between groups were considered statistically significant with a P value cutoff of ≤ 0.05 . Data are represented as means \pm SEM. In all cases, ****, $P \leq 0.0001$; ***, $P \leq 0.001$; **, $P \leq 0.01$; *, $P \leq 0.05$; ns, not statistically significant ($P > 0.05$); and ND, not detectable/below limit of detection.

RNA-seq and computational analysis

Cell sorting

Spleens (days 0, 5, and 10), spinal cord (day 10), and brain (day 10) were dissected from mice that were challenged with EAE. Single-cell suspensions were described as above. Spleen cells were resuspended in MACS buffer (DPBS, 2% FBS, and 2 mM EDTA) and further enriched for CD4 T cells using the Dynabeads Flowcomp mouse CD4 kit (Life Technologies). For the day 10 time point, cells were pooled from two to three mice for each sample. The enriched cells were stained with fluorochrome-conjugated anti-CD45.2, anti-TCR β , anti-CD4, anti-CD44, anti-CD62L, anti-ST2, anti-CD11b, anti-CD8, anti-B220, and anti-NK1.1 (dump gate) before sorting on a BD FACSAria II sorter. Cells were sorted into TRIzol LS (Life Technologies). Cells were sorted in triplicate as CD44⁺CD62L⁻CD4⁺Foxp3⁻ T eff cells (spleen, days 0, 5, and 10, 10^5 cells each; CNS, day 10, 2.75×10^4 to 10^5), as CD44⁺CD62L⁻CD4⁺Foxp3⁺ T reg cells (spleen, days 0, 5, and 10, 10^5 cells each; CNS, day 10, 0.9×10^4 to 3×10^4), and as CD45^{int}CD11b⁺ microglia (CNS, day 10, 8.8×10^4 to 10^5). For a representative gating strategy, please refer to Fig. S3 F.

Computational analysis

RNA-seq reads were aligned to the reference mouse genome GRCm38 using the STAR RNA-seq aligner, and local realignment was performed using the Genome Analysis Toolkit (Dobin et al., 2013; McKenna et al., 2010). For each sample, the raw count of reads per gene was measured using R, and the DESeq2 R package was used to perform differential gene expression between WT and KO in each cell type (Love et al., 2014). A cutoff of 0.05 was set on the P values (adjusted using Benjamini-Hochberg multiple testing correction) to get the significant genes of each comparison. The threshold to minimum average expression within samples of each comparison was set to 30 reads. Volcano plots and heatmaps were constructed using R. For PCA analysis, the 15,000 most variant genes were included in the calculation of components, and 3D plots were made using the plot3d R package. Gene ontology analysis was performed using gene set enrichment analysis software, and all biological functions, hallmark genesets, and KEGG pathways were ranked by normalized enrichment score, after a false discovery rate cutoff of

≤ 0.25 was applied (Subramanian et al., 2005). Associated plots were also constructed using R.

Data availability

The RNA-seq data has been made publicly available in the Sequence Read Archive database and can be accessed under accession no. PRJNA648990.

Online supplemental material

Fig. S1 shows that ST2 expression on T cells promotes antiviral T cell response against LCMV. Fig. S2 shows that T reg cell-specific loss of the signaling adapter MyD88 affects body weight and adipose tissue immune cell composition. Fig. S3 shows that IL-33 protein is elevated in the spinal cord of symptomatic mice and correlates with progressive accumulation of ST2-expressing T reg cells in EAE.

Acknowledgments

We thank A. Bravo, M. Faire, and J. Verter for help with animal husbandry. We thank all the members of the Rudensky laboratory for discussion and advice.

This work was supported by the National Institutes of Health/National Cancer Institute Cancer Center Support Grant P30 CA008748, National Institutes of Health grant AI034206, and the Ludwig Center at the Memorial Sloan Kettering Cancer Center. A.Y. Rudensky is an investigator with the Howard Hughes Medical Institute.

Author contributions: S. Hemmers and A.Y. Rudensky conceptualized the study, designed experiments, and interpreted all the data. S. Hemmers performed all experiments and prepared the figures for publication. M. Schizas performed bioinformatic analyses and data visualization of the RNA-seq data with supervision and input from S. Hemmers. S. Hemmers and A.Y. Rudensky wrote the manuscript with input from co-authors. A.Y. Rudensky supervised and acquired funding for the study.

Disclosures: A.Y. Rudensky reported personal fees from Sonoma Biotherapeutics outside the submitted work. No other disclosures were reported.

Submitted: 15 June 2020

Revised: 11 August 2020

Accepted: 16 September 2020

References

- Ali, N., B. Zirak, R.S. Rodriguez, M.L. Pauli, H.A. Truong, K. Lai, R. Ahn, K. Corbin, M.M. Lowe, T.C. Scharschmidt, et al. 2017. Regulatory T Cells in Skin Facilitate Epithelial Stem Cell Differentiation. *Cell*. 169: 1119–1129.e11. <https://doi.org/10.1016/j.cell.2017.05.002>
- Allan, D., K.J. Fairlie-Clarke, C. Elliott, C. Schuh, S.C. Barnett, H. Lassmann, C. Linnington, and H.R. Jiang. 2016. Role of IL-33 and ST2 signalling pathway in multiple sclerosis: expression by oligodendrocytes and inhibition of myelination in central nervous system. *Acta Neuropathol. Commun.* 4:75. <https://doi.org/10.1186/s40478-016-0344-1>
- Arpaia, N., J.A. Green, B. Molledo, A. Arvey, S. Hemmers, S. Yuan, P.M. Treuting, and A.Y. Rudensky. 2015. A Distinct Function of Regulatory T Cells in Tissue Protection. *Cell*. 162:1078–1089. <https://doi.org/10.1016/j.cell.2015.08.021>

- Bapat, S.P., J. Myoung Suh, S. Fang, S. Liu, Y. Zhang, A. Cheng, C. Zhou, Y. Liang, M. LeBlanc, C. Liddle, et al. 2015. Depletion of fat-resident Treg cells prevents age-associated insulin resistance. *Nature*. 528:137–141. <https://doi.org/10.1038/nature16151>
- Bennett, C.L., J. Christie, F. Ramsdell, M.E. Brunkow, P.J. Ferguson, L. Whitesell, T.E. Kelly, F.T. Saulsbury, P.F. Chance, and H.D. Ochs. 2001. The immune dysregulation, polyendocrinopathy, enteropathy, X-linked syndrome (IPEX) is caused by mutations of FOXP3. *Nat. Genet.* 27:20–21. <https://doi.org/10.1038/83713>
- Blink, S.E., M.W. Caldis, G.E. Goings, C.T. Harp, B. Malissen, I. Prinz, D. Xu, and S.D. Miller. 2014. $\gamma\delta$ T cell subsets play opposing roles in regulating experimental autoimmune encephalomyelitis. *Cell. Immunol.* 290:39–51. <https://doi.org/10.1016/j.cellimm.2014.04.013>
- Bonilla, W.V., A. Fröhlich, K. Senn, S. Kallert, M. Fernandez, S. Johnson, M. Kreuzfeldt, A.N. Hegazy, C. Schrick, P.G. Fallon, et al. 2012. The alarmin interleukin-33 drives protective antiviral CD8⁺ T cell responses. *Science*. 335:984–989. <https://doi.org/10.1126/science.1215418>
- Brestoff, J.R., B.S. Kim, S.A. Saenz, R.R. Stine, L.A. Monticelli, G.F. Sonnenberg, J.J. Thome, D.L. Farber, K. Lutfy, P. Seale, and D. Artis. 2015. Group 2 innate lymphoid cells promote being of white adipose tissue and limit obesity. *Nature*. 519:242–246. <https://doi.org/10.1038/nature14115>
- Brunkow, M.E., E.W. Jeffery, K.A. Hjerrild, B. Paeper, L.B. Clark, S.A. Yaszko, J.E. Wilkinson, D. Galas, S.F. Ziegler, and F. Ramsdell. 2001. Disruption of a new forkhead/winged-helix protein, scurfy, results in the fatal lymphoproliferative disorder of the scurfy mouse. *Nat. Genet.* 27:68–73. <https://doi.org/10.1038/83784>
- Burzyn, D., W. Kuswanto, D. Kolodin, J.L. Shadrach, M. Cerletti, Y. Jang, E. Sefik, T.G. Tan, A.J. Wagers, C. Benoist, and D. Mathis. 2013. A special population of regulatory T cells potentiates muscle repair. *Cell*. 155:1282–1295. <https://doi.org/10.1016/j.cell.2013.10.054>
- Carriere, V., L. Roussel, N. Ortega, D.A. Lacorre, L. Americh, L. Aguilar, G. Bouche, and J.P. Girard. 2007. IL-33, the IL-1-like cytokine ligand for ST2 receptor, is a chromatin-associated nuclear factor in vivo. *Proc. Natl. Acad. Sci. USA*. 104:282–287. <https://doi.org/10.1073/pnas.0606854104>
- Cayrol, C., and J.P. Girard. 2018. Interleukin-33 (IL-33): A nuclear cytokine from the IL-1 family. *Immunol. Rev.* 281:154–168. <https://doi.org/10.1111/imr.12619>
- Chen, C.C., T. Kobayashi, K. Iijima, F.C. Hsu, and H. Kita. 2017. IL-33 dysregulates regulatory T cells and impairs established immunologic tolerance in the lungs. *J. Allergy Clin. Immunol.* 140:1351–1363.e7. <https://doi.org/10.1016/j.jaci.2017.01.015>
- Chen, H., Y. Sun, L. Lai, H. Wu, Y. Xiao, B. Ming, M. Gao, H. Zou, P. Xiong, Y. Xu, et al. 2015. Interleukin-33 is released in spinal cord and suppresses experimental autoimmune encephalomyelitis in mice. *Neuroscience*. 308:157–168. <https://doi.org/10.1016/j.neuroscience.2015.09.019>
- Cipolletta, D., M. Feuerer, A. Li, N. Kamei, J. Lee, S.E. Shoelson, C. Benoist, and D. Mathis. 2012. PPAR- γ is a major driver of the accumulation and phenotype of adipose tissue Treg cells. *Nature*. 486:549–553. <https://doi.org/10.1038/nature11132>
- Delacher, M., C.D. Imbusch, A. Hotz-Wagenblatt, J.P. Mallm, K. Bauer, M. Simon, D. Riegel, A.F. Rendeiro, S. Bittner, L. Sanderink, et al. 2020. Precursors for Nonlymphoid-Tissue Treg Cells Reside in Secondary Lymphoid Organs and Are Programmed by the Transcription Factor BATF. *Immunity*. 52:295–312.e11. <https://doi.org/10.1016/j.immuni.2019.12.002>
- Dobin, A., C.A. Davis, F. Schlesinger, J. Drenkow, C. Zaleski, S. Jha, P. Batut, M. Chaisson, and T.R. Gingeras. 2013. STAR: ultrafast universal RNA-seq aligner. *Bioinformatics*. 29:15–21. <https://doi.org/10.1093/bioinformatics/bts635>
- Dogan, R.N., N. Long, E. Forde, K. Dennis, A.P. Kohm, S.D. Miller, and W.J. Karpus. 2011. CCL22 regulates experimental autoimmune encephalomyelitis by controlling inflammatory macrophage accumulation and effector function. *J. Leukoc. Biol.* 89:93–104. <https://doi.org/10.1189/jlb.0810442>
- Dombrowski, Y., T. O'Hagan, M. Dittmer, R. Penalva, S.R. Mayoral, P. Bankhead, S. Fleville, G. Eleftheriadis, C. Zhao, M. Naughton, et al. 2017. Regulatory T cells promote myelin regeneration in the central nervous system. *Nat. Neurosci.* 20:674–680. <https://doi.org/10.1038/nn.4528>
- El-Behi, M., B. Ciric, H. Dai, Y. Yan, M. Cullimore, F. Safavi, G.X. Zhang, B.N. Dittel, and A. Rostami. 2011. The encephalitogenicity of T(H)17 cells is dependent on IL-1- and IL-23-induced production of the cytokine GM-CSF. *Nat. Immunol.* 12:568–575. <https://doi.org/10.1038/ni.2031>
- Fairlie-Clarke, K., M. Barbour, C. Wilson, S.U. Hridi, D. Allan, and H.R. Jiang. 2018. Expression and Function of IL-33/ST2 Axis in the Central Nervous System Under Normal and Diseased Conditions. *Front. Immunol.* 9:2596. <https://doi.org/10.3389/fimmu.2018.02596>
- Feurerer, M., L. Herrero, D. Cipolletta, A. Naaz, J. Wong, A. Nayer, J. Lee, A.B. Goldfine, C. Benoist, S. Shoelson, and D. Mathis. 2009. Lean, but not obese, fat is enriched for a unique population of regulatory T cells that affect metabolic parameters. *Nat. Med.* 15:930–939. <https://doi.org/10.1038/nm.2002>
- Fontenot, J.D., M.A. Gavin, and A.Y. Rudensky. 2003. Foxp3 programs the development and function of CD4⁺CD25⁺ regulatory T cells. *Nat. Immunol.* 4:330–336. <https://doi.org/10.1038/ni904>
- Gadani, S.P., J.T. Walsh, I. Smirnov, J. Zheng, and J. Kipnis. 2015. The gliaderived alarmin IL-33 orchestrates the immune response and promotes recovery following CNS injury. *Neuron*. 85:703–709. <https://doi.org/10.1016/j.neuron.2015.01.013>
- Goverman, J. 2009. Autoimmune T cell responses in the central nervous system. *Nat. Rev. Immunol.* 9:393–407. <https://doi.org/10.1038/nri2550>
- Guo, L., G. Wei, J. Zhu, W. Liao, W.J. Leonard, K. Zhao, and W. Paul. 2009. IL-1 family members and STAT activators induce cytokine production by Th2, Th17, and Th1 cells. *Proc. Natl. Acad. Sci. USA*. 106:13463–13468. <https://doi.org/10.1073/pnas.0906988106>
- Guo, X.J., P. Dash, J.C. Crawford, E.K. Allen, A.E. Zamora, D.F. Boyd, S. Duan, R. Bajracharya, W.A. Awad, N. Apiwattanakul, et al. 2018. Lung $\gamma\delta$ T Cells Mediate Protective Responses during Neonatal Influenza Infection that Are Associated with Type 2 Immunity. *Immunity*. 49:531–544.e6. <https://doi.org/10.1016/j.immuni.2018.07.011>
- Han, J.M., D. Wu, H.C. Denroche, Y. Yao, C.B. Verchere, and M.K. Levings. 2015. IL-33 Reverses an Obesity-Induced Deficit in Visceral Adipose Tissue ST2⁺ T Regulatory Cells and Ameliorates Adipose Tissue Inflammation and Insulin Resistance. *J. Immunol.* 194:4777–4783. <https://doi.org/10.4049/jimmunol.1500020>
- Hou, B., B. Reizis, and A.L. DeFranco. 2008. Toll-like receptors activate innate and adaptive immunity by using dendritic cell-intrinsic and -extrinsic mechanisms. *Immunity*. 29:272–282. <https://doi.org/10.1016/j.immuni.2008.05.016>
- Hövelmeyer, N., F.T. Wunderlich, R. Massoumi, C.G. Jakobsen, J. Song, M.A. Wörns, C. Merkwirth, A. Kovalenko, M. Aumailley, D. Strand, et al. 2007. Regulation of B cell homeostasis and activation by the tumor suppressor gene CYLD. *J. Exp. Med.* 204:2615–2627. <https://doi.org/10.1084/jem.20070318>
- Ito, M., K. Komai, S. Mise-Omata, M. Iizuka-Koga, Y. Noguchi, T. Kondo, R. Sakai, K. Matsuo, T. Nakayama, O. Yoshie, et al. 2019. Brain regulatory T cells suppress astroglia and potentiate neurological recovery. *Nature*. 565:246–250. <https://doi.org/10.1038/s41586-018-0824-5>
- Jiang, H.R., M. Milovanović, D. Allan, W. Niedbala, A.G. Besnard, S.Y. Fukada, J.C. Alves-Filho, D. Togbe, C.S. Goodyear, C. Linington, et al. 2012. IL-33 attenuates EAE by suppressing IL-17 and IFN- γ production and inducing alternatively activated macrophages. *Eur. J. Immunol.* 42:1804–1814. <https://doi.org/10.1002/eji.201141947>
- Josefowicz, S.Z., L.F. Lu, and A.Y. Rudensky. 2012. Regulatory T cells: mechanisms of differentiation and function. *Annu. Rev. Immunol.* 30:531–564. <https://doi.org/10.1146/annurev.immunol.25.022106.141623>
- Khattri, R., T. Cox, S.A. Yaszko, and F. Ramsdell. 2003. An essential role for Scurfin in CD4⁺CD25⁺ T regulatory cells. *Nat. Immunol.* 4:337–342. <https://doi.org/10.1038/ni909>
- Kim, J.M., J.P. Rasmussen, and A.Y. Rudensky. 2007. Regulatory T cells prevent catastrophic autoimmunity throughout the lifespan of mice. *Nat. Immunol.* 8:191–197. <https://doi.org/10.1038/ni1428>
- Kohlgruber, A.C., S.T. Gal-Oz, N.M. LaMarche, M. Shimazaki, D. Duquette, H.F. Koay, H.N. Nguyen, A.I. Mina, T. Paras, A. Tavakkoli, et al. 2018. $\gamma\delta$ T cells producing interleukin-17A regulate adipose regulatory T cell homeostasis and thermogenesis. *Nat. Immunol.* 19:464–474. <https://doi.org/10.1038/s41590-018-0094-2>
- Kolodin, D., N. van Panhuys, C. Li, A.M. Magnuson, D. Cipolletta, C.M. Miller, A. Wagers, R.N. Germain, C. Benoist, and D. Mathis. 2015. Antigen- and cytokine-driven accumulation of regulatory T cells in visceral adipose tissue of lean mice. *Cell Metab.* 21:543–557. <https://doi.org/10.1016/j.cmet.2015.03.005>
- Koutrolos, M., K. Berer, N. Kawakami, H. Wekerle, and G. Krishnamoorthy. 2014. Treg cells mediate recovery from EAE by controlling effector T cell proliferation and motility in the CNS. *Acta Neuropathol. Commun.* 2:163. <https://doi.org/10.1186/s40478-014-0163-1>
- Kurowska-Stolarska, M., P. Kewin, G. Murphy, R.C. Russo, B. Stolarski, C.C. Garcia, M. Komai-Koma, N. Pitman, Y. Li, W. Niedbala, et al. 2008. IL-33 induces antigen-specific IL-5⁺ T cells and promotes allergic-induced airway inflammation independent of IL-4. *J. Immunol.* 181:4780–4790. <https://doi.org/10.4049/jimmunol.181.7.4780>

- Kuswanto, W., D. Burzyn, M. Panduro, K.K. Wang, Y.C. Jang, A.J. Wagers, C. Benoist, and D. Mathis. 2016. Poor Repair of Skeletal Muscle in Aging Mice Reflects a Defect in Local, Interleukin-33-Dependent Accumulation of Regulatory T Cells. *Immunity*. 44:355–367. <https://doi.org/10.1016/j.immuni.2016.01.009>
- Lahl, K., C. Loddenkemper, C. Drouin, J. Freyer, J. Arnason, G. Eberl, A. Hamann, H. Wagner, J. Huehn, and T. Sparwasser. 2007. Selective depletion of Foxp3+ regulatory T cells induces a scurfy-like disease. *J. Exp. Med.* 204:57–63. <https://doi.org/10.1084/jem.20061852>
- Lee, P.P., D.R. Fitzpatrick, C. Beard, H.K. Jessup, S. Lehar, K.W. Makar, M. Pérez-Melgosa, M.T. Sweetser, M.S. Schlissel, S. Nguyen, et al. 2001. A critical role for Dnmt1 and DNA methylation in T cell development, function, and survival. *Immunity*. 15:763–774. [https://doi.org/10.1016/S1074-7613\(01\)00227-8](https://doi.org/10.1016/S1074-7613(01)00227-8)
- Li, C., J.R. DiSpirito, D. Zemmour, R.G. Spallanzani, W. Kuswanto, C. Benoist, and D. Mathis. 2018. TCR Transgenic Mice Reveal Stepwise, Multi-site Acquisition of the Distinctive Fat-Treg Phenotype. *Cell*. 174:285–299.e12. <https://doi.org/10.1016/j.cell.2018.05.004>
- Li, M., Y. Li, X. Liu, X. Gao, and Y. Wang. 2012. IL-33 blockade suppresses the development of experimental autoimmune encephalomyelitis in C57BL/6 mice. *J. Neuroimmunol.* 247:25–31. <https://doi.org/10.1016/j.jneuroim.2012.03.016>
- Liang, Y., Z. Jie, L. Hou, R. Aguilar-Valenzuela, D. Vu, L. Soong, and J. Sun. 2013. IL-33 induces neutrophils and modulates liver injury in viral hepatitis. *J. Immunol.* 190:5666–5675. <https://doi.org/10.4049/jimmunol.1300117>
- Liu, Q., G.K. Dwyer, Y. Zhao, H. Li, L.R. Mathews, A.B. Chakka, U.R. Chandran, J.A. Demetris, J.F. Alcorn, K.M. Robinson, et al. 2019. IL-33-mediated IL-13 secretion by ST2+ Tregs controls inflammation after lung injury. *JCI Insight*. 4:e123919.
- Love, M.I., W. Huber, and S. Anders. 2014. Moderated estimation of fold change and dispersion for RNA-seq data with DESeq2. *Genome Biol.* 15: 550. <https://doi.org/10.1186/s13059-014-0550-8>
- Mahlköv, T., A.L. Flamar, L.K. Johnston, S. Moriyama, G.G. Putzel, P.J. Bryce, and D. Artis. 2019. Stromal cells maintain immune cell homeostasis in adipose tissue via production of interleukin-33. *Sci. Immunol.* 4: eaax0416. <https://doi.org/10.1126/sciimmunol.aax0416>
- Matta, B.M., J.M. Lott, L.R. Mathews, Q. Liu, B.R. Rosborough, B.R. Blazar, and H.R. Turnquist. 2014. IL-33 is an unconventional Alarmin that stimulates IL-2 secretion by dendritic cells to selectively expand IL-33R/ST2+ regulatory T cells. *J. Immunol.* 193:4010–4020. <https://doi.org/10.4049/jimmunol.1400481>
- McGinley, A.M., C.E. Sutton, S.C. Edwards, C.M. Leane, J. DeCoursey, A. Teijeiro, J.A. Hamilton, L. Boon, N. Djouder, and K.H.G. Mills. 2020. Interleukin-17A Serves a Priming Role in Autoimmunity by Recruiting IL-1 β -Producing Myeloid Cells that Promote Pathogenic T Cells. *Immunity*. 52:342–356.e6. <https://doi.org/10.1016/j.immuni.2020.01.002>
- McKenna, A., M. Hanna, E. Banks, A. Sivachenko, K. Cibulskis, A. Kernytsky, K. Garimella, D. Altshuler, S. Gabriel, M. Daly, and M.A. DePristo. 2010. The Genome Analysis Toolkit: a MapReduce framework for analyzing next-generation DNA sequencing data. *Genome Res.* 20:1297–1303. <https://doi.org/10.1101/gr.107524.110>
- Miller, A.M., D.L. Asquith, A.J. Hueber, L.A. Anderson, W.M. Holmes, A.N. McKenzie, D. Xu, N. Sattar, I.B. McInnes, and F.Y. Liew. 2010. Interleukin-33 induces protective effects in adipose tissue inflammation during obesity in mice. *Circ. Res.* 107:650–658. <https://doi.org/10.1161/CIRCRESAHA.110.218867>
- Milovanovic, M., V. Volarevic, B. Ljubic, G. Radosavljevic, I. Jovanovic, N. Arsenijevic, and M.L. Lukic. 2012. Deletion of IL-33R (ST2) abrogates resistance to EAE in BALB/C mice by enhancing polarization of APC to inflammatory phenotype. *PLoS One*. 7:e45225. <https://doi.org/10.1371/journal.pone.0045225>
- Miragaia, R.J., T. Gomes, A. Chomka, L. Jardine, A. Riedel, A.N. Hegazy, N. Whibley, A. Tucci, X. Chen, I. Lindeman, et al. 2019. Single-Cell Transcriptomics of Regulatory T Cells Reveals Trajectories of Tissue Adaptation. *Immunity*. 50:493–504.e7. <https://doi.org/10.1016/j.immuni.2019.01.001>
- Mohri, I., M. Taniike, H. Taniguchi, T. Kanekiyo, K. Aritake, T. Inui, N. Fukumoto, N. Eguchi, A. Kushi, H. Sasai, et al. 2006. Prostaglandin D2-mediated microglia/astrocyte interaction enhances astrogliosis and demyelination in twitcher. *J. Neurosci.* 26:4383–4393. <https://doi.org/10.1523/JNEUROSCI.4531-05.2006>
- Molofsky, A.B., F. Van Gool, H.E. Liang, S.J. Van Dyken, J.C. Nussbaum, J. Lee, J.A. Bluestone, and R.M. Locksley. 2015. Interleukin-33 and Interferon- γ Counter-Regulate Group 2 Innate Lymphoid Cell Activation during Immune Perturbation. *Immunity*. 43:161–174. <https://doi.org/10.1016/j.immuni.2015.05.019>
- Morita, H., K. Arae, H. Unno, K. Miyauchi, S. Toyama, A. Nambu, K. Oboki, T. Ohno, K. Motomura, A. Matsuda, et al. 2015. An Interleukin-33-Mast Cell-Interleukin-2 Axis Suppresses Papain-Induced Allergic Inflammation by Promoting Regulatory T Cell Numbers. *Immunity*. 43:175–186. <https://doi.org/10.1016/j.immuni.2015.06.021>
- Moussion, C., N. Ortega, and J.P. Girard. 2008. The IL-1-like cytokine IL-33 is constitutively expressed in the nucleus of endothelial cells and epithelial cells in vivo: a novel ‘alarmin’? *PLoS One*. 3:e3331. <https://doi.org/10.1371/journal.pone.0003331>
- Panduro, M., C. Benoist, and D. Mathis. 2016. Tissue Tregs. *Annu. Rev. Immunol.* 34:609–633. <https://doi.org/10.1146/annurev-immunol-032712-095948>
- Petermann, F., V. Rothhammer, M.C. Claussen, J.D. Haas, L.R. Blanco, S. Heink, I. Prinz, B. Hemmer, V.K. Kuchroo, M. Oukka, and T. Korn. 2010. $\gamma\delta$ T cells enhance autoimmunity by restraining regulatory T cell responses via an interleukin-23-dependent mechanism. *Immunity*. 33: 351–363. <https://doi.org/10.1016/j.immuni.2010.08.013>
- Pichery, M., E. Mirey, P. Mercier, E. Lefrancais, A. Dujardin, N. Ortega, and J.P. Girard. 2012. Endogenous IL-33 is highly expressed in mouse epithelial barrier tissues, lymphoid organs, brain, embryos, and inflamed tissues: in situ analysis using a novel IL-33-LacZ gene trap reporter strain. *J. Immunol.* 188:3488–3495. <https://doi.org/10.4049/jimmunol.1101977>
- Rajan, A.J., J.D. Klein, and C.F. Brosnan. 1998. The effect of gammadelta T cell depletion on cytokine gene expression in experimental allergic encephalomyelitis. *J. Immunol.* 160:5955–5962.
- Rothhammer, V., J.E. Kenison, E. Tjon, M.C. Takenaka, K.A. de Lima, D.M. Borucki, C.C. Chao, A. Wilz, M. Blain, L. Healy, et al. 2017. Sphingosine 1-phosphate receptor modulation suppresses pathogenic astrocyte activation and chronic progressive CNS inflammation. *Proc. Natl. Acad. Sci. USA*. 114:2012–2017. <https://doi.org/10.1073/pnas.1615413114>
- Rubtsov, Y.P., J.P. Rasmussen, E.Y. Chi, J. Fontenot, L. Castelli, X. Ye, P. Treuting, L. Siewe, A. Roers, W.R. Henderson Jr., et al. 2008. Regulatory T cell-derived interleukin-10 limits inflammation at environmental interfaces. *Immunity*. 28:546–558. <https://doi.org/10.1016/j.immuni.2008.02.017>
- Sakaguchi, S., N. Mikami, J.B. Wing, A. Tanaka, K. Ichiyama, and N. Ohkura. 2020. Regulatory T Cells and Human Disease. *Annu. Rev. Immunol.* 38: 541–566. <https://doi.org/10.1146/annurev-immunol-042718-041717>
- Sakaguchi, S., N. Sakaguchi, M. Asano, M. Itoh, and M. Toda. 1995. Immunologic self-tolerance maintained by activated T cells expressing IL-2 receptor α -chains (CD25). Breakdown of a single mechanism of self-tolerance causes various autoimmune diseases. *J. Immunol.* 155: 1151–1164.
- Sandler, N.G., M.M. Mentink-Kane, A.W. Cheever, and T.A. Wynn. 2003. Global gene expression profiles during acute pathogen-induced pulmonary inflammation reveal divergent roles for Th1 and Th2 responses in tissue repair. *J. Immunol.* 171:3655–3667. <https://doi.org/10.4049/jimmunol.171.7.3655>
- Scheiblich, H., M. Trombly, A. Ramirez, and M.T. Heneka. 2020. Neuro-immune Connections in Aging and Neurodegenerative Diseases. *Trends Immunol.* 41:300–312. <https://doi.org/10.1016/j.it.2020.02.002>
- Schiering, C., T. Krausgruber, A. Chomka, A. Fröhlich, K. Adelman, E.A. Wohlfert, J. Pott, T. Griseri, J. Bollrath, A.N. Hegazy, et al. 2014. The alarmin IL-33 promotes regulatory T-cell function in the intestine. *Nature*. 513:564–568. <https://doi.org/10.1038/nature13577>
- Schmitz, J., A. Owyang, E. Oldham, Y. Song, E. Murphy, T.K. McClanahan, G. Zurawski, M. Moshrefi, J. Qin, X. Li, et al. 2005. IL-33, an interleukin-1-like cytokine that signals via the IL-1 receptor-related protein ST2 and induces T helper type 2-associated cytokines. *Immunity*. 23:479–490. <https://doi.org/10.1016/j.immuni.2005.09.015>
- Siede, J., A. Fröhlich, A. Datsi, A.N. Hegazy, D.V. Varga, V. Holeccka, H. Saito, S. Nakae, and M. Löhning. 2016. IL-33 Receptor-Expressing Regulatory T Cells Are Highly Activated, Th2 Biased and Suppress CD4 T Cell Proliferation through IL-10 and TGF β Release. *PLoS One*. 11:e0161507. <https://doi.org/10.1371/journal.pone.0161507>
- Spahn, T.W., S. Issazadah, A.J. Salvin, and H.L. Weiner. 1999. Decreased severity of myelin oligodendrocyte glycoprotein peptide 33 - 35-induced experimental autoimmune encephalomyelitis in mice with a disrupted TCR delta chain gene. *Eur. J. Immunol.* 29:4060–4071. [https://doi.org/10.1002/\(SICI\)1521-4141\(199912\)29:12<4060::AID-IMMU4060>3.0.CO;2-S](https://doi.org/10.1002/(SICI)1521-4141(199912)29:12<4060::AID-IMMU4060>3.0.CO;2-S)
- Spallanzani, R.G., D. Zemmour, T. Xiaoy, T. Jayewickreme, C. Li, P.J. Bryce, C. Benoist, and D. Mathis. 2019. Distinct immunocyte-promoting and

- adipocyte-generating stromal components coordinate adipose tissue immune and metabolic tenors. *Sci. Immunol.* 4:eaaw3658. <https://doi.org/10.1126/sciimmunol.aaw3658>
- Stromnes, I.M., and J.M. Goverman. 2006. Active induction of experimental allergic encephalomyelitis. *Nat. Protoc.* 1:1810–1819. <https://doi.org/10.1038/nprot.2006.285>
- Subramanian, A., P. Tamayo, V.K. Mootha, S. Mukherjee, B.L. Ebert, M.A. Gillette, A. Paulovich, S.L. Pomeroy, T.R. Golub, E.S. Lander, and J.P. Mesirov. 2005. Gene set enrichment analysis: a knowledge-based approach for interpreting genome-wide expression profiles. *Proc. Natl. Acad. Sci. USA.* 102:15545–15550. <https://doi.org/10.1073/pnas.0506580102>
- Sutton, C.E., S.J. Lalor, C.M. Sweeney, C.F. Brereton, E.C. Lavelle, and K.H. Mills. 2009. Interleukin-1 and IL-23 induce innate IL-17 production from gammadelta T cells, amplifying Th17 responses and autoimmunity. *Immunity.* 31:331–341. <https://doi.org/10.1016/j.immuni.2009.08.001>
- Turnquist, H.R., Z. Zhao, B.R. Rosborough, Q. Liu, A. Castellaneta, K. Isse, Z. Wang, M. Lang, D.B. Stolz, X.X. Zheng, et al. 2011. IL-33 expands suppressive CD11b⁺ Gr-1(int) and regulatory T cells, including ST2L⁺ Foxp3⁺ cells, and mediates regulatory T cell-dependent promotion of cardiac allograft survival. *J. Immunol.* 187:4598–4610. <https://doi.org/10.4049/jimmunol.1100519>
- Vasanthakumar, A., D. Chisanga, J. Blume, R. Gloury, K. Britt, D.C. Henstridge, Y. Zhan, S.V. Torres, S. Liene, N. Collins, et al. 2020. Sex-specific adipose tissue imprinting of regulatory T cells. *Nature.* 579:581–585. <https://doi.org/10.1038/s41586-020-2040-3>
- Vasanthakumar, A., K. Moro, A. Xin, Y. Liao, R. Gloury, S. Kawamoto, S. Fagarasan, L.A. Mielke, S. Afshar-Sterle, S.L. Masters, et al. 2015. The transcriptional regulators IRF4, BATF and IL-33 orchestrate development and maintenance of adipose tissue-resident regulatory T cells. *Nat. Immunol.* 16:276–285. <https://doi.org/10.1038/ni.3085>
- Xiao, Y., L. Lai, H. Chen, J. Shi, F. Zeng, J. Li, H. Feng, J. Mao, F. Zhang, N. Wu, et al. 2018. Interleukin-33 deficiency exacerbated experimental autoimmune encephalomyelitis with an influence on immune cells and glia cells. *Mol. Immunol.* 101:550–563. <https://doi.org/10.1016/j.molimm.2018.08.026>
- Yasuoka, S., J. Kawanokuchi, B. Parajuli, S. Jin, Y. Doi, M. Noda, Y. Sonobe, H. Takeuchi, T. Mizuno, and A. Suzumura. 2011. Production and functions of IL-33 in the central nervous system. *Brain Res.* 1385:8–17. <https://doi.org/10.1016/j.brainres.2011.02.045>

Supplemental material

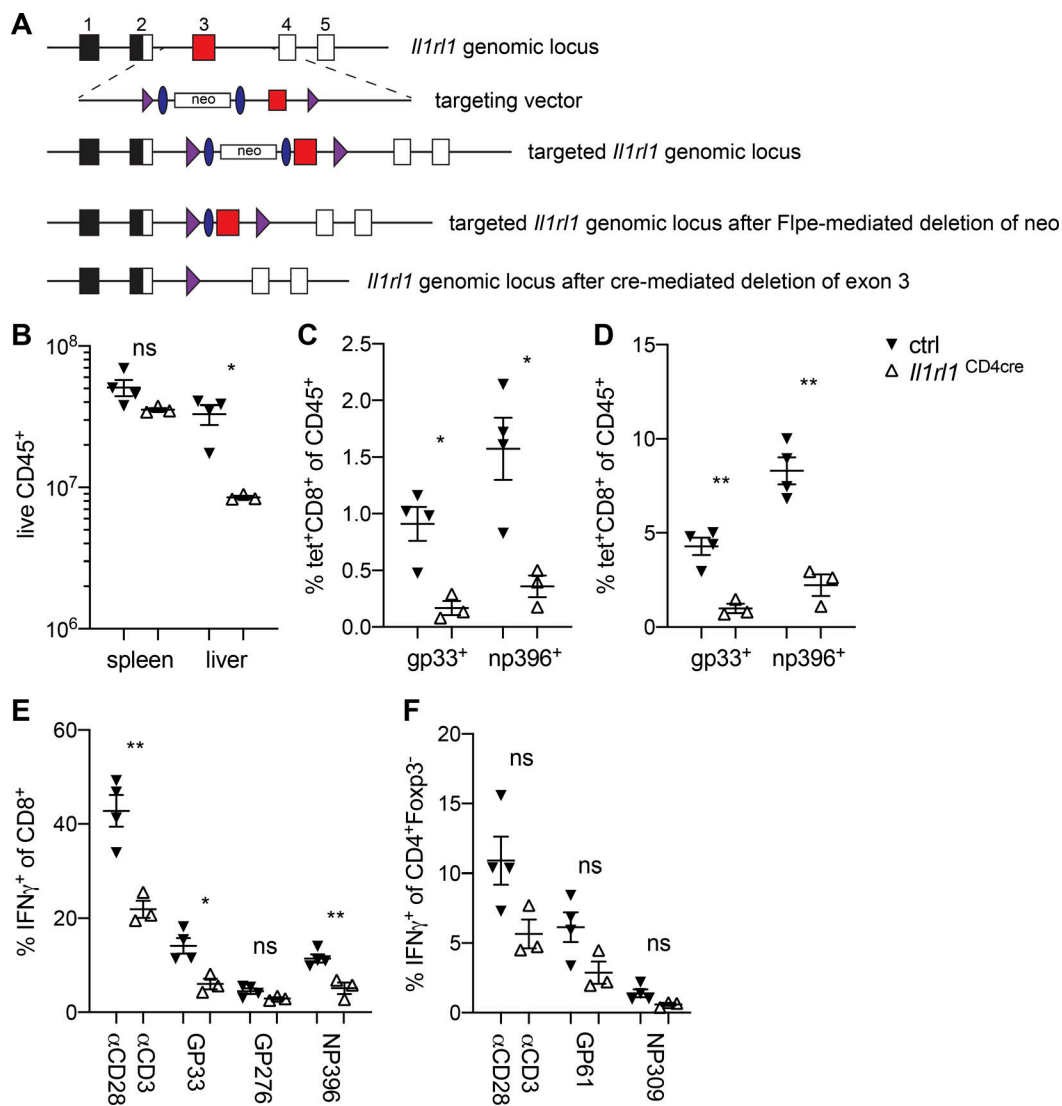


Figure S1. **ST2 expression on T cells promotes antiviral T cell response against LCMV.** (A) Schematic overview of generation of a novel conditional KO allele for ST2. *loxP* sites (purple triangles) were introduced into the genomic *Il1rl1* locus to flank exon 3 (red box) by homologous recombination in embryonic stem cells. The targeting vector contained a neo cassette flanked by *frt* sites (blue ovals) to allow for selection of successful recombination at the locus. The neomycin selection cassette was removed by breeding mice that carried the recombinant allele in their germline with a FLPe-deleter strain. The *Il1rl1*^{fl} allele was subsequently intercrossed with *Foxp3*^{yfpcre} or CD4-cre mice to specifically restrict ST2 deletion to T reg cells in the former and all T cells in the latter by cre recombinase-mediated excision of the *loxP* flanked exon 3. (B-F) Control (ctrl; n = 4; black triangles) and *Il1rl1*^{CD4cre} mice (n = 3; white triangles) were infected with 2 × 10⁵ PFU LCMV Armstrong. All data shown here are from day 7 after infection, including total immune cell numbers in spleen and liver (B). LCMV-specific CD8 T cells were quantified in spleen (C) and liver (D) using tetramers detecting cells responding to the virus-derived peptides GP33 and NP396. Production of IFN γ by CD8 (E) and CD4 (F) T cells was assessed after ex vivo stimulation with α CD3/ α CD28 or LCMV-derived peptides. Data in B-F are plotted as means ± SEM and representative of two independent experiments. **, P ≤ 0.01; *, P ≤ 0.05; ns, P > 0.05 by unpaired t test.

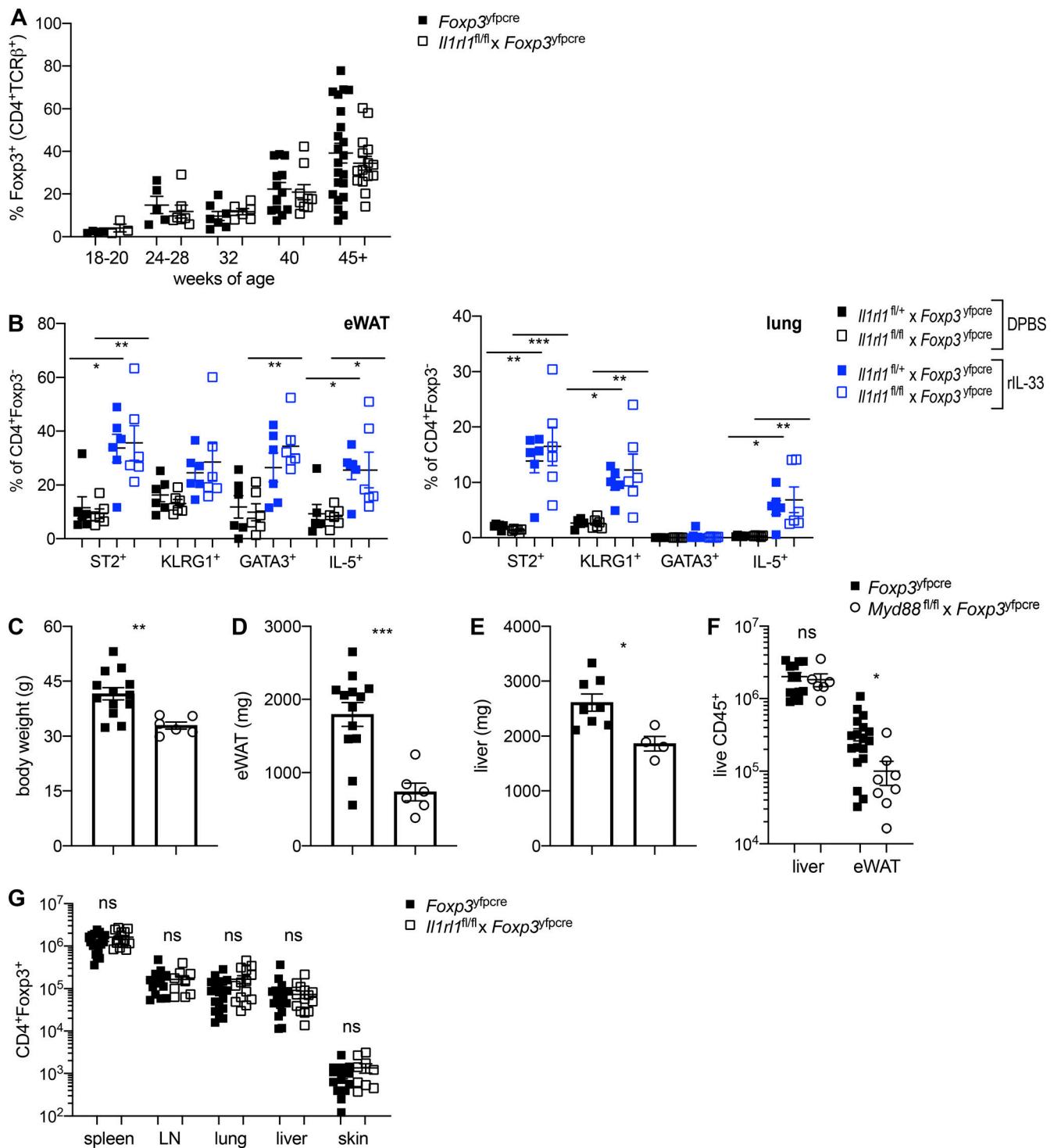


Figure S2. T reg cell-specific loss of the signaling adapter MyD88 affects body weight and adipose tissue immune cell composition. (A) T reg cell frequencies in adipose tissue are plotted for individual mice of the indicated ages. (B) Mice received either DPBS or 500 ng of recombinant mouse IL-33 i.p. as indicated. Frequency of ST2-, KLRG1-, GATA3-, or IL-5-expressing CD4⁺ T cells in eWAT (left) or lung (right) contrasting *Il1rl1^{fl/+} x Foxp3^{yfpcre}* (*n* = 6; DPBS, black filled squares; IL-33, black open squares) and *Il1rl1^{fl/fl} x Foxp3^{yfpcre}* mice (*n* = 6; DPBS, blue filled squares; IL-33, blue open squares) are plotted. (C–G) All data were collected from 11–13-mo-old male mice. Total body weight (C), eWAT weight (D), and liver weight (E) are plotted for individual mice. (F) Quantification of immune cells in liver and eWAT from *Foxp3^{yfpcre}* (*n* = 8–18; black squares) or *Myd88^{fl/fl} x Foxp3^{yfpcre}* mice (*n* = 4–8; open circles). (G) Absolute numbers of T reg cells in lymphoid and nonlymphoid tissues of *Foxp3^{yfpcre}* (*n* = 19; black squares) or *Il1rl1^{fl/fl} x Foxp3^{yfpcre}* mice (*n* = 9–14; open squares). Data in A–G are plotted as means ± SEM and are pooled from two to four independent experiments. ***, *P* ≤ 0.001; **, *P* ≤ 0.01; *, *P* ≤ 0.05; ns > 0.05 by one-way ANOVA with Sidak’s multiple comparisons correction (B) or unpaired *t* test (A and C–G). For clarity, only comparisons that were significantly different are indicated in B.

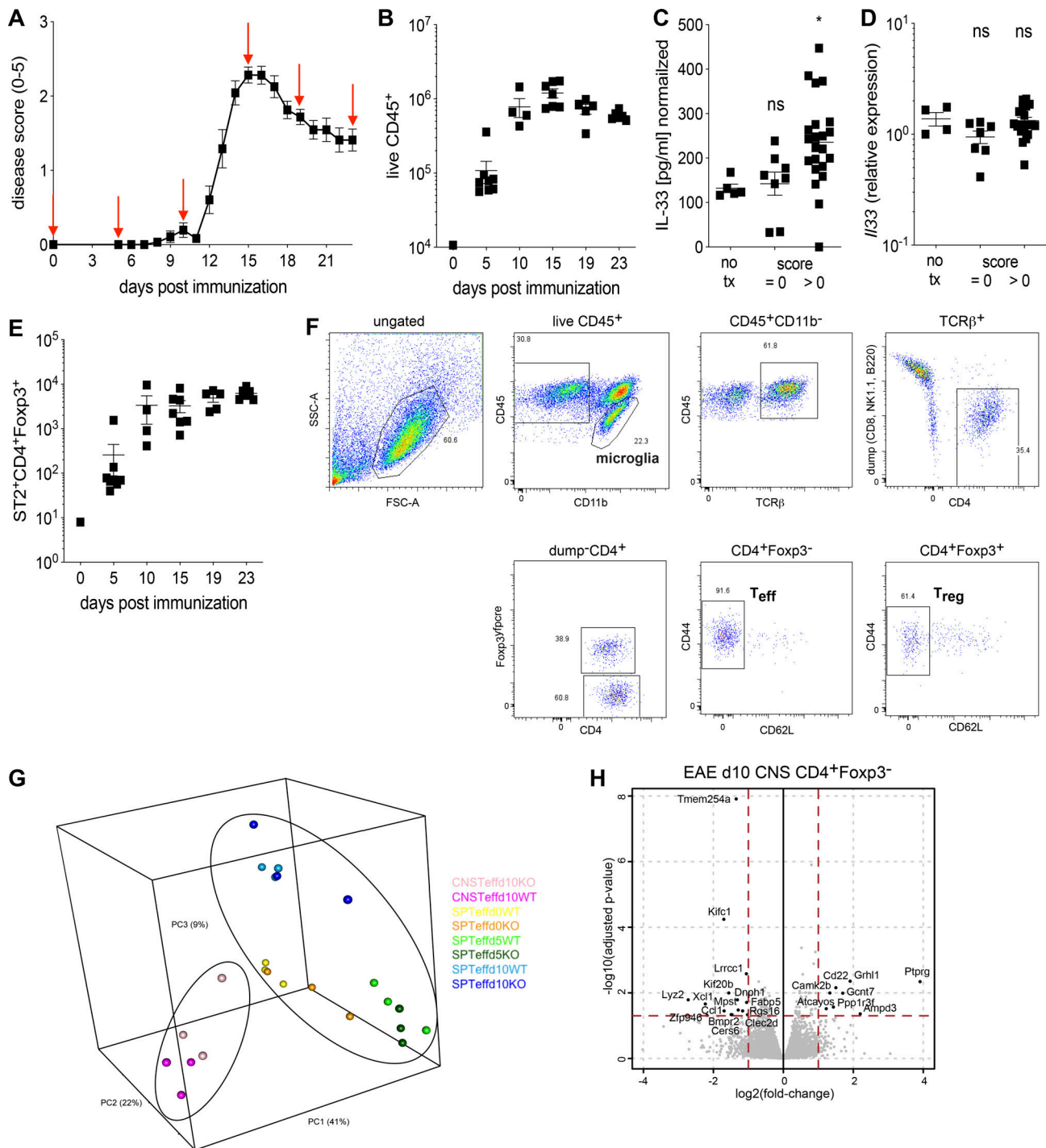


Figure S3. IL-33 protein is elevated in the spinal cord of symptomatic mice and correlates with progressive accumulation of ST2-expressing T reg cells in EAE. (A) C57BL/6 mice ($n = 35$; black squares) were immunized with MOG peptide in CFA to induce EAE. Disease progression was assessed on a daily basis and is plotted as a disease score. Mice were sampled at various stages of disease (red arrows) as follows: day 0 ($n = 5$), day 5 ($n = 8$), day 10 ($n = 4$), day 15 ($n = 7$), day 19 ($n = 5$), and day 23 ($n = 6$). (B) Total immune cell infiltration into the CNS was enumerated over the disease course and is plotted for individual mice. (C and D) IL-33 protein content (C) and *Il33* transcript levels (D) were quantified in the spinal cord of naive mice (no treatment [tx]; $n = 5$), asymptomatic mice (score = 0; $n = 7-8$), and symptomatic mice (score > 0; $n = 20-22$). (E) Total numbers of ST2-expressing T reg cells in the CNS are plotted for individual mice over the course of disease. (F) A typical gating strategy is shown exemplifying how microglia (live CD45^{int}CD11b⁺), T eff cells (dump⁻CD4⁺Foxp3⁻CD62L⁻CD44⁺), and T reg cells (dump⁻CD4⁺Foxp3⁺CD62L⁻CD44⁺) were sorted from CNS for subsequent RNA-seq analysis at day 10 after EAE induction. FSC, forward scatter; SSC, side scatter. (G) 3D PCA of CD4 T eff cells from spleen (days 0, 5, and 10) and CNS (day 10). (H) Volcano plot of gene expression data contrasting T eff cells isolated from the CNS at day 10 after EAE induction from *Foxp3^{yfpcre}* (WT) or *Il1rl1^{fl/fl} × Foxp3^{yfpcre}* (KO) mice. Genes with a FC ≥ 2 and an adjusted P value < 0.05 are labeled. Genes increased in KO are on the left and genes decreased in KO are on the right of the plot. Data in C and D are representative of two independent experiments. Data in A–E are plotted as means \pm SEM. *, $P \leq 0.05$; ns, $P > 0.05$ by unpaired *t* test. PC, principal component.